TECHNISCHE UNIVERSITÄT WIEN
Vienna University of Technology

DIPLOMARBEIT

Analyse der Deltaregelzone mit Fokus auf erneuerbare Energieerzeugung

zur Erlangung des akademischen Grades

Diplom - Ingenieurin

im Rahmen des Masterstudiums

Statistik-Wirtschaftsmathematik

eingereicht von

Barbara Keck, BSc

Matrikelnummer: 01225589

Durchgeführt am Institut für Stochastik und Wirtschaftsmathematik, an der Fakultät für Mathematik und Geoinformation, an der Technischen Universität Wien.

Betreuung:
Ao.Univ.Prof. Wolfgang Scherrer

Wien, am 16.09.2021

Betreuer | Autorin

Affidavit

I declare in lieu of oath that the present work was prepared by me independently in accordance with the recognized principles for scientific treatises. All aids used, in particular the literature on which they are based, are named and listed in this work. The passages taken verbatim from the sources are marked as such.

So far, I have not presented the topic of this work to an appraiser for assessment in any form as an examination paper, either at home or abroad. This work agrees with the work assessed by the assessors.

Place, Date	Barbara Keck, BSc

A note of thanks

I would not be where I am right now, if I had not gotten the support of so many people. Now is the time to thank all of them.

First, but without implying any particular order, I want to express my deepest gratitude to all these wonderful people (some of them older, some of them younger) that are part of my family. With some being there with me since my first moments, and some of them joining later down the road, all of them contributed to making me the person I am today. Thank you - and if you read this you know that I'm talking about you here - for the support, the encouragement, always being there for me, making the right decisions when I could not and for every fun minute we had together (which means all of them).

A huge thank you goes to all of my friends, to people who have joined me on the way and were there for me during difficult times. Without them, studying and the life outside university would have been only half the fun. Whether it was learning together for exams, preparing exercises, having fun in the evening or at the weekends. They made this period of life an experience. Thank you for all of that!

I want to thank my better half, who always supports me through challenging times and really helped me to stay focused on my studies, which were not always easy for me. I am really happy to have you at my side.

Finally I want to express my gratitude to Prof. Scherrer for supervising my thesis and for always having a word of advice. The topic of this thesis originated in talks with the E-Control - thanks for that.

Without all of this support, this thesis would not have been possible.

Barbara Keck
Vienna, September 2021

Abstract

Background: On January 8, 2021 a power outage in almost all of Transylvania/Romania led to a critical drop in frequency. For the first time since November 4, 2006 the normal range was undercut with 49.746 Hz. Incidents like this make an analysis of balancing energy demand inevitable. *Method:* A two-stage model was developed. In stage I, an attempt is made to predict the absolute load, solar and wind forecast errors. Then the results of the first stage are used as explanatory variables for the analysis of the absolute control area imbalance in stage II. *Results:* Using a two-stage modelling approach proves to be beneficial, mostly due to the fact that the absolute wind forecast error shows a significant influence on the absolute control area imbalance. The final results of a model utilizing only quantile regression showcase a stable performance in all comparisons and a reduction in MAE and RMSE by 11% and 5% respectively when compared to the best performing benchmark (a mean forecast).

Zusammenfassung

Hintergrund: Am 8. Januar 2021 führte ein Stromausfall in fast ganz Siebenbürgen/Rumänien zu einem kritischen Frequenzabfall. Zum ersten Mal seit dem 4. November 2006 wurde der Normalbereich mit 49,746 Hz unterschritten. Störungen dieser Art machen eine Analyse des Regenlenergiebedafs unumgänglich. *Methode:* Es wurde ein zweistufiges Modell entwickelt. In Stufe I werden mathematische Modelle entwickelt um die absoluten Last-, Solar- und Windprognosefehler zu beschreiben. Die Ergebnisse der ersten Stufe werden als erklärende Variablen für die Analyse des absoluten Wertes der Deltaregelzone in Stufe II verwendet. *Ergebnisse:* Die Verwendung eines zweistufigen Modellierungsansatzes erweist sich als vorteilhaft, hauptsächlich aufgrund der Tatsache, dass der absolute Windprognosefehler einen signifikanten Einfluss auf den absoluten Wert der Deltaregelzone hat. Die Ergebnisse des Modells, das ausschließlich Quantile Regression verwendet, zeigen eine stabile Leistung in allen Vergleichen und eine Verringerung von MAE und RMSE um 11% bzw. 5% im Vergleich zum Benchmark mit der besten Leistung (eine Durchschnittsprognose).

Contents

Chapter 1

Introduction

In Austria, the liberalization of the electricity and natural gas markets took place in 2001 and 2002. Clear rules were required for all market participants, so that fair competition could develop in the electricity market. As a regulatory authority in Austria, the legislator established the E-Control on the basis of the Energy Regulatory Authorities Act, which is now responsible for establishing and verifying these regulations. It is their task as regulator to monitor the implementation of the liberalization of the Austrian electricity and gas market, to accompany and, if necessary, to intervene and regulate.
The regulation has two components: the ex-ante regulation, through which the framework conditions or rules under which competition is to take place are set before trading, and the ex-post regulation, through which competition violations can be identified and eliminated. With the instrument of market monitoring, E-Control is able to follow and analyze developments in the market.

In June 2019 there was an enormous electricity bottleneck in Germany. On three days in 2019, the four transmission system operators (TSOs) in Germany only managed to prevent a widespread collapse of the power supply with great effort. The reason for this was that forecasts of the power supply were off by such a large margin that it became necessary several times to feed large amounts of balancing energy into the grid in order to prevent a widespread collapse of the power grid.
Research into the causes goes in two directions: on the one hand, the forecast errors and breaches of duty in the involved balancing groups concerned and, on the other hand, any market manipulation that may be present by the market participants. This is just one of many events, which can also occur in Austria,

where a large amount of balancing energy is required [Röhrlich, 2019].

On January 8, 2021 a power outage in almost all of Transylvania/Romania led to a critical drop in frequency. For the first time since November 4, 2006 the normal range (49.8 - 50.2 Hz) was undercut with 49.746 Hz and thus this represents the second most major disturbance ever in the European network system, since 2006.
The European power grid is normally synchronized to compensate for any fluctuations (most of the time the Frequency Containment Reserve (FCR) is enough). If the frequency falls too low, this synchronization will be interrupted automatically. So-called temporary network splitting occurs, in which the network is split up. There are a number of security mechanisms that take effect in such a case. In order for the frequency to slip back into the normal range, reserves of several power plants were activated (also in Austria). After about an hour, the normal state was restored [Futurezone, 2021].

In this thesis the focus is on forecast errors as well as on the control area imbalance and therefore the recent developments in the electricity market are examined. During the last few years there have been a lot of developments in the electricity market, which affect the requirements of balancing energy. Rising CO_2 emissions and global warming led to an expansion of renewable and sustainable forms of energy generation. In particular, electricity generation through wind and solar systems has become increasingly important. Measures like these are undoubtedly necessary. However renewable forms of energy are coupled with an increased volatility, which further increases the demand of balancing energy.
The exact demand of balancing energy is difficult to predict. In the context of this thesis, the preparation and mathematical analysis of given input data (such as wind and solar forecast data as well as supply and demand data on the Austrian electricity market) should be carried out as well as their connection with the forecast error (for renewable energies; subsequently the forecast of the need for of balancing energy) on the electricity market.

The aim is to create a day ahead forecast for the absolute control area imbalance where the absolute load, solar and wind forecast errors are used as explanatory variables. In the first chapter, details on balancing energy are explained in order to provide an understanding of the following analysis. In this context there are also scientific papers presented in the section called "State of the Art". Next, a

descriptive statistical analysis of the given data (ranging from 2015 to 2020) is carried out.
The results of the descriptive analysis will show it is reasonably to restrict the data to the years 2019 and 2020. The data from 2019 are used for modeling the three different absolute forecast errors (load, solar, wind) as well as the control area imbalance and those from 2020 are used as test data to check the quality of the different modeled forecasts.
The model is developed in two stages. In the first stage, the model deals with the analysis of the absolute forecast error of load, solar and wind and uses a multiple linear regression, a tobit model (only for the solar forecast error) and a quantile regression. Then the results of the first stage (for the predicted absolute load, solar and wind forecast errors) are used as an input factor for the analysis of the absolute control area imbalance in the second stage. All results (both stages) are documented in this thesis.

Chapter 2

Basic Explanations

The energy system is a network of different actors. Supply and demand are created by producers and consumers. The exchange of electricity takes place through the transmission network, which joins all participants. An essential property of electricity grids is that electricity cannot be stored, except for small storages in form of batteries, or large storages in different forms of energy (e.g. potential energy of pumped water). In order to make electricity available for the consumers, certain framework conditions must be adhered to, e.g. the grid frequency must always be at 50 Hz. This is only possible as long as the amount fed in is equal to the amount withdrawn.

There exists free competition in Austria concerning power generation, trading and sales, and there is a so-called "balancing group system" defined. A balancing group is the combination of suppliers and customers in a virtual group within which there is a balance between supply and demand. As long as this balance is achieved, even if there are some deviations from planned set-points, no balancing energy from the control area is activated. A control area can consist of many balancing groups. Every market participant is obliged to join a balancing group. The Austrian Power Grid is the transmission system operator (TSO) and has a monopoly position. The TSO is responsible for the proper metering of feed-in and consumption, the confidential administration of the data as well as the balanced operation of the specific control area. Balancing energy is provided by qualified producers, and organized by the TSO through an auction process.

2.1 Renewable Energies on the Austrian Electricity Market

The generation mix of Austrian power plants is characterized by renewable energies and in particular by clean hydropower. The flexible mix is complemented by highly efficient thermal power plants. Due to this, in comparison to other European countries, Austria is one of the countries with the lowest emissions per kWh. With a share of 60.5%, hydropower is the most important source of electricity in Austria. The second pillar of the flexible Austrian energy mix are thermal power plants with a share of 24%. New renewable forms of energy - such as wind, solar and geothermal energy - are making an increasing contribution to domestic electricity generation [Österreichs E-Wirtschaft, 2018].
Austria's first wind turbine went online in 1994, but it took until 2002 for the expansion of wind power to really get started. From then on, a separate green electricity law regulated electricity generation by wind turbines. The first expansion phase was from 2002 until 2006. The expansion further continued since 2012 due to the Green Electricity Act. Currently, in Austria every year around 63 TWh of electricity are consumed. At the end of 2017, wind turbines provided an annual generation of 7 TWh, that is 11% of the domestic electricity demand. In a second expansion phase, wind power output doubled in just four years. The total installed capacity by the end of 2020 was 3198 MW [ENTSO-E, 2020a], [InteressengemeinschaftWindkraft, 2020], [WienEnergie, 2019].
The Austrian government itself has set the goal of covering 100 percent (nationally balanced) of electricity consumption in Austria from renewable energy sources by 2030. Accordingly, by 2030, enough solar power is to be added that 11 TWh will come from solar systems. This will increase the installed solar capacity from currently 1851 MW (2021) to around 13 GW - within the next 10 years [APG, 2020].

2.2 Balancing Energy

Balancing energy is a reserve to compensate fluctuations in the electricity grid. These fluctuations are expressed in a decrease or increase in the power grid frequency of nominally 50 Hz. When using balancing energy, electricity can both be taken from the power grid (negative balancing energy) as well as supplied (positive balancing energy). Balancing energy can be provided by power generation systems and electricity storage systems, negative balancing energy can also be provided by electricity consumers.

The expansion of renewable energies leads to fluctuations in the electricity grid due to the growing influence of wind and solar energy. Not only the weather, but also electricity consumers cause fluctuations due to irregular demand profiles. Nevertheless, power outages are very rare in Austria - thanks to the balancing energy and an ever better forecast quality for power generation and consumption.
At the same time, an increasing share of electricity power plants in Austria are able to quickly provide large amounts of balancing power as Frequency Containment Reserve (FCR), Automatic Frequency Restoration Reserve (aFRR) and Manual Frequency Restoration Reserve (mFRR) . While the FCR is balanced continuously and within seconds based on a grid frequency measurement, the TSO issues call-up commands for the aFRR and the mFRR, which must be answered by the connected systems within 5 or 15 minutes, respectively [Kraftwerke, 2020].

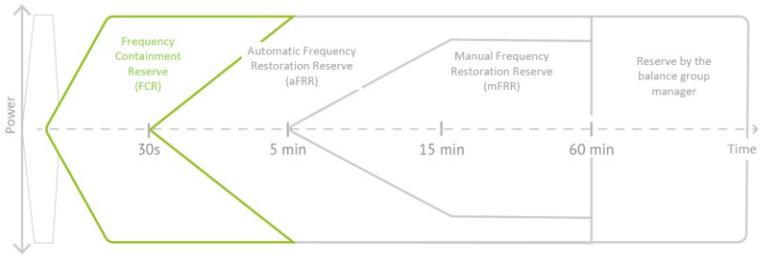

Figure 2.1: Timing - Austrian Frequency Reserve [Kraftwerke, 2020]

The quantities of balancing energy are subject to certain conditions to ensure the proper operation of the control area. The Austrian control area is linked to other control areas in Europe. This enables the exchange of electricity between the different zones in Europe. The result is that imbalances in one control area are carried over to others. The FCR is therefore used or made available by all members of the European Network. Activation takes place automatically depending on the measured network frequency and independent of the source. In contrast, the aFRR and the mFRR are activated in control areas with persistent imbalances. Therefore, the focus in this thesis is on the analysis of the quantities of aFRR and mFRR.

Situations that require balancing energy are difficult to predict. If that were not the case, it would be possible to include the necessary amount of electricity

in the standard planning. There are many discussions why the total amount of necessary balancing energy did not increase proportionally to the share of renewable energies in the electricity grid. Therefore the question about the reasons why and when there is a need for balancing energy arises.
This thesis aims to analyze the various dependencies and effects of given input parameters (like renewable forecasts, load forecasts and power exchange prices) on the needed quantity of aFRR and mFRR (the sum being called "control area imbalance") in the Austrian control area managed by the Austrian Power Grid AG (APG). Due to technical and economic reasons, as already mentioned above, balancing energy is divided into three categories [APG, 2020]:

1. Frequency Containment Reserve (= "Primärregelreserve")

   The FCR is provided by power plants and is required to automatically compensate for an imbalance between generation and consumption within a few seconds through appropriate activation and thus to stabilize the frequency in the connected power grid. The FCR is automatically activated through the use of turbine regulators in power plants - based on the respective operating point. The activation is triggered by deviations of the frequency from the setpoint (50 Hz), whereby the activated FCR also increases with increasing frequency deviation. The maximum activation occurs with a frequency deviation of 200 mHz and above - the FCR is then exhausted. The maximum activation must be achieved no later than 30 seconds after the occurrence of the corresponding frequency deviation.

2. Automatic Frequency Restoration Reserve (= "Sekundärregelreserve")

   The aFRR is required to relieve the activated FCR and again ensure its future availability. The aFRR is activated automatically so that the FCR is relieved and free so that it can again fulfill its function of network balancing. The aFRR is activated if the influence on the network lasts longer than 30 seconds or it is assumed that it will last longer than 30 seconds. Before that, the deviation of the network is only covered by the FCR.

3. Manual Frequency Restoration Reserve (= "Tertiärregelreserve")

   The mFRR is activated if the deviation in the control area lasts longer than 15 minutes. The mFRR is used to relieve the aFRR so that it is free again in order to support the FCR or make it available again if necessary. The mFRR can be activated automatically or manually.

The control area imbalance [APG, 2020] is the surplus or deficit of electrical energy in the control area. It equals the sum of all balancing group deviations (balancing energy) and is calculated as sum of the following components:

- aFRR and mFRR,
- Unintended exchange [1] with the continental European synchronous network.

2.3 Separation of the Germany-Austria Electricity Price Zone

In May 2017, the German and Austrian regulatory authorities (BNetzA and E-Control) agreed to separate the common electricity price zone[2] that has existed since the electricity market was liberalized. As the TSO, the APG is responsible for the technical implementation of this decision. The separation of the Germany-Austria electricity price zone came into effect on October 1, 2018. Since that day, the cross-border exchange of electricity is no longer possible without restrictions as before, but is guaranteed up to the extent of 4.9 GWh. This corresponds to around half of the Austrian consumption at peak times [APG, 2020].

2.4 Power Exchanges

Whether electricity is needed for the current (intraday (ID)) or the following day (day ahead (DA)), EPEX Spot (spot market of the European Power Exchange) is the leading energy exchange for spot markets. EPEX Spot covers the markets in France, Germany, Austria and Switzerland. Together these countries already consume more than a third of the overall European electricity. The company is based in Paris and has branches in Leipzig, Bern and Vienna. The following two sections explain the timings and deadlines for the different products in more detail.

[1] These are deviations between the setpoint and actual values of the exchange between neighboring power grids. The unintentional exchange of the control area is the amount of energy that the control area takes from the grid area of the Regional Group Continental Europe or is delivered to it. [APG, 2020]

[2] A bidding zone - also known as the electricity price zone - is the largest geographical area in which electricity can be traded on the wholesale market without capacity allocation. The assumption is that no bottlenecks occur within a bidding zone, so the exchange of energy is possible without restrictions. This means that there is a uniform market price within a bidding zone. [APG, 2020]

2.4.1 Day Ahead

Definition

The term day ahead trading refers to the trading of electricity for the following day, which takes place on the EPEX Spot in Paris, on the EXAA in Vienna (Energy Exchange Austria) or in the form of OTC (over-the-counter trading) trades, which take place via contracts negotiated outside of exchanges. The term auction market is also used sometimes [Kraftwerke, 2020].

Timing

The EPEX spot market is divided into four different market regions: France, Switzerland, Germany and Austria. For the individual market regions, trading is again differentiated according to the respective transmission system operator. In the German and Austrian markets, the bids for the auctions for the next day must be submitted by 12 noon. The market results are published at 12:40 p.m. each day [Kraftwerke, 2020].

2.4.2 Intraday

Definition

Intraday electricity trading takes place both on spot markets such as the EPEX Spot and in OTC trading, i.e. via contracts negotiated outside of exchanges between electricity buyers and sellers. It describes the continuous purchase and sale of electricity that is delivered on the same day. That is called a short-term electricity wholesale, especially in contrast to electricity trading with longer lead times on the futures market [Kraftwerke, 2020].

Timing

In short-term continuous electricity trading, electricity deliveries are usually traded in both 15-minute and hourly blocks. It is also possible to trade larger blocks. The possibility of quarter-hourly trading is probably the most important characteristic of intraday trading. A position can be traded up to 5 minutes before delivery begins. Intraday trading opens at 3 p.m. the previous day. At this time, the continuous trading of hourly products and, since December 9, 2014, the opening auction of quarter-hour products will start. The latter then be traded continuously for the following day from 4 p.m.

One difference to day ahead trading is the price formation on the intraday market: While day ahead trading is always based on the principle of the market-clearing price, in which the last bid that was accepted determines the price ("marginal pricing") for all transactions ("Merit-Order principle" [3]), the prices in continuous intraday trading are determined using the "pay-as-bid" method [Kraftwerke, 2020].

[3] A merit order is the order in which the units in a power plant system are used. This order is determined by the marginal costs of the individual power generator.

Chapter 3

State of the Art

In this section, scientific work will be presented that has dealt with the modeling of balancing energy in recent years. Due to constant regulatory changes in the electricity markets and thus also in the markets for balancing energy in recent years, there are a variety of approaches to estimate the maximum demand of balancing energy. This is necessary for TSOs to safely procure enough balancing capacity, in order to ensure grid stability at (almost) all times. A short presentation of different approaches to estimate sensible upper bounds of this demand for balancing energy seems useful. In general one can choose between static and dynamic, as well as between deterministic (heuristic) and probabilistic methods in order to estimate the needed balancing energy. As a reminder, the aFRR and mFRR are part of the control area imbalance. Therefore, the procured quantity of these products plays a role in the consideration and analysis of the control area imbalance.

3.1 Methods to estimate Balancing Demand

In contrast to the determination of the aFRR and mFRR, the need for FCR is determined at the European level. The failure of 3000 MW of generation or consumption is assumed as a reference incident for the continental European area. The demand of FCR is allocated to the TSOs of the area on the basis of an annually recalculated distribution key. The annual net electricity generation and the annual net electricity consumption in the control area are decisive for this [Amprion, 2020]. A distinction is made between different methods to estimate the needed balancing energy. These methods are explained in more detail below.

3.1.1 Static Approaches

Static approaches define the balancing energy to be provided for longer periods of time and do not take into account any forecasts for changing influencing factors within these periods. Thus the result is a static value for the entire period. An example of a static algorithm is the Graf-Haubrich method. In Germany, aFRR and mFRR are provided by the TSOs. The amount tendered is determined every three months for the upcoming three months using the Graf-Haubrich method to dimension the balancing energy demand based on the errors that occurred in the previous twelve months. The idea behind this method is that the various errors that occur (which lead to a need of balancing energy) belong to an overall error distribution. In this way, the control power requirement can be determined [Jansen, 2014], [Jost et al., 2015a].

3.1.2 Dynamic Approaches

Dynamic approaches take changing influences on the balancing energy demand within the periods for which the estimation is carried out into account. At the same time, these periods are significantly shorter. E.g. estimation takes place once a day for the following day, whereby a constant value for each hour is set. In research these dynamic methods gain in importance due to their advantages with high proportions of fluctuating feed-in, e.g. because of wind or solar power [Jost et al., 2015a].

3.1.3 Deterministic (heuristic) Approaches

Some deterministic approaches define the demand of balancing energy to be kept available based on a specific event that is to be controlled, such as for example the failure of the largest power plant or another component (called n-1 criterion). When estimating the FCR in Central Europe for example the simultaneous failure of the two largest power plants with the amount of 3000 MW is the reference incident that should be controlled with the help of the FCR.
Heuristic methods are based on empirical values, e.g. a certain percentage of the annual maximum load. However, it does not take into account how often the reserve is not sufficient or what proportion of the required balancing energy can actually be covered, which is a serious disadvantage compared to probabilistic procedures [Jost et al., 2015a].

3.1.4 Probabilistic Approaches

Probabilistic approaches assume an acceptable probability of grid failure. The probabilistic method can basically choose between simulative and statistical methods.
Simulative methods simulate the behavior of individual components within the energy supply system and consider failures with certain probabilities. An example for this method is the Monte Carlo Simulation.
Statistical processes determine the demand of balancing energy on the basis of historical data. The most simple method is to measure the balancing energy used over a certain period of time and then to use this to determine a probability distribution of the balancing energy calls. In the Graf-Haubrich method (used in Germany), the probability distributions for different errors such as power plant failures, load forecast errors, etc. are determined and then folded into an overall error distribution under the assumption of stochastic independence [Jost et al., 2015a].

3.2 Econometrics and Time Series Analysis

Econometrics and time series analysis are common tools in the context of the balancing energy market. In [Wenzel, 2011] the sum of aFRR and mFRR together was considered. The sum was analyzed by splitting it into a trend-component, two periodic components (with an hourly and daily period) and a remainder term, that was modeled using an ARIMA model. In [Möller et al., 2011] not the amount of balancing energy but instead imbalances (inside balance groups) are considered. This is closely related, but not identical. A detailed explanation about the difference can be found in [E-Control, 2020]. The focus in [Möller et al., 2011] is on the consideration of the residuals in the context of SARIMA models of time series, including the implementation of forecasts as well as the evaluation of the forecasts. In [Kurscheid and Düvelmeyer, 2009] calls of mFRR are modeled as a Poisson process.
It should be mentioned that during recent years methods of econometrics and time series analysis are often used in the context of balancing energy market analysis. In addition to econometric models, alternative probabilistic approaches to determine the balancing energy are developed.
In recent years the framework conditions of the electricity markets and thus also the markets for balancing energy have been subject to constant changes and

there is a variety of approaches to model and estimate the need for balancing energy. In this thesis the focus is not on the estimation of the total procured balancing reserve but rather on modeling the time series of the control area imbalance (and thus modeling the time series of the sum of aFRR and mFRR) and their dependencies on other factors such as renewable energies.

3.3 Different Types of Regression Analysis

In the area of the balancing energy market, the influence of renewable energies plays an increasingly important role. That explains why the influence wind and solar generation on the balancing energy market is being examined more intensively. For example [Abuella and Chowdhury, 2015] proposes a multiple linear regression to generate probabilistic forecasts for solar energy.
The load forecast is also often examined using a multiple linear regression. For example in [Amral et al., 2007] an investigation of the short term (up to 24 hours) load forecasting of the demand for the South Sulewesi's (Sulewesi Island - Indonesia) power system is considered using multiple linear regression. Historical data is used (hourly load and temperatures) to forecast the short term load.
In [Abuella and Chowdhury, 2017] the solar energy is considered too. This paper presents a support vector regression to produce solar power forecasts on a rolling basis for 24 hours ahead over an entire year, with the aim to mimic the practical business of energy forecasting. Then there is a comparison made with artificial neuronal networks and multiple linear regression for energy forecasting. Countless other papers can be found on the subject of multiple linear regression concerning the energy market.
In [Tsekouras et al., 2007] the authors describe a non-linear multivariable regression for midterm energy forecasting of power systems in an annual time base. In addition to (non-linear) multiple linear regression and vector regression, other models can also be used. Although tobit models are rarely used concerning the energy market, [Singhee and Wang, 2017] developed a tobit model applicable to severe weather events.
In contrast to ordinary least squares estimation (OLS), the quantile regression - as a method of estimating the parameters of a regression model - considers the quantiles of the conditional distribution of the dependent variable given the independent variable. In [Wan et al., 2016] a novel direct quantile regression approach to efficiently generate nonparametric probabilistic forecasting of wind power generation combining extreme learning machine and quantile regression

is suggested. Also in [Bracale et al., 2019] a new cooperative forecasting system that refines probabilistic forecasts of individual loads online is proposed. As mentioned in the paper the refining procedure is based on a multivariate quantile regression, which is dynamically applied to the individual forecasts as new observations become available.

Chapter 4

Descriptive Analysis

This chapter deals with the amount of the activated balancing energy in the control area in the years 2015 to 2020, with the exception of FCR. The reason for the neglect of the FCR is that FCR is not part of the control area imbalance. Besides, the FCR is also used in the entire European network as first instance for the balanced operation of the power grid. On the other hand, aFRR and mFRR are activated specifically in the control area that caused the electricity deficit or the excess of electricity [E-Control, 2020].
It should be mentioned that in the analysis only the consolidated amount of aFRR and mFRR is considered. This consolidated amount (plus unintended exchange) is also called "control area imbalance". This happens for the reason that both forms of balancing energy pursue the same goal - to compensate deviations in the control area. Even though these balancing energy markets have different technical characteristics and are traded separately, there is always a physical need for constant balance between electricity supply and demand, which is fulfilled by both products.

4.1 Data Sources

All data that is used must be available on the day ahead. The data was taken from the ENTSO-E and APG homepage [APG, 2020], [ENTSO-E, 2020b]. The dataset includes 52608 observations of 75 different variables in the period from January 1^{st}, 2015 to December 31^{st}, 2020. About 30 variables of the 71 variables are examined more closely. Hourly data, which was originally recorded in quarter-hourly steps, was generated by aggregation into hours with the aid of averaging. That concerns the data of the load (load forecast and actual load)

and renewable energies (forecast and actual generation). In this thesis only the data for Austria is considered.
The data can be divided into the following groups:

- Control area imbalance (sum of aFRR and mFRR including the unintended exchange)
- Load (actual load and forecast)
- Solar (actual generation and forecast)
- Wind (actual generation and forecast)
- Day ahead price

4.2 Control Area Imbalance

The data on the control area imbalance was taken from the APG website [APG, 2020]. A distinction is made between operational and billing-relevant data. The operational and billing-relevant data differ only slightly. Since values of the operational data are available for all years from 2015 onwards (in comparison to the billing-relevant data), the decision was made to work with the operational data of the control area imbalance.
In figure 4.1 and 4.2 the control area imbalance starting from 2015 to 2020 is shown, once grouped per hour and once per month. In either plot, no large differences between hours respectively months can be observed.
In figure 4.3 the autocorrelation of the operational data of the control area imbalance (2015 to 2020) can be seen. It suggests a weak autocorrelation.

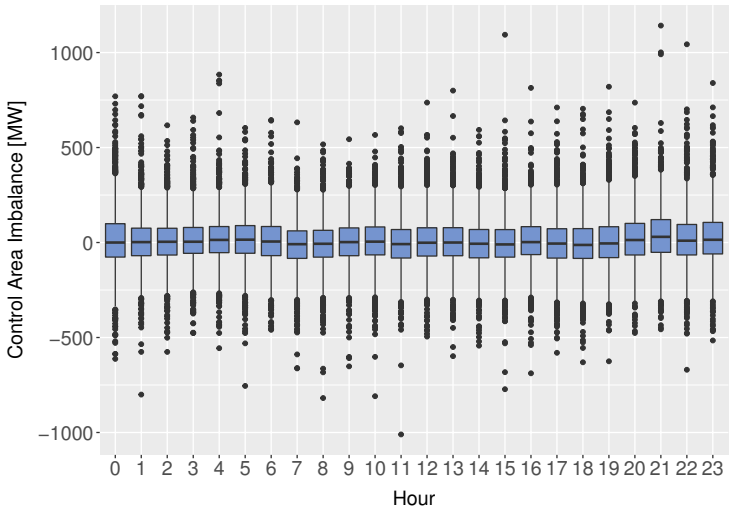

Figure 4.1: Control area imbalance during the years 2015 - 2020. Boxplots grouped per hour. Some hours exhibit more extreme outliers with values ranging up/down to +/-1000 MW.

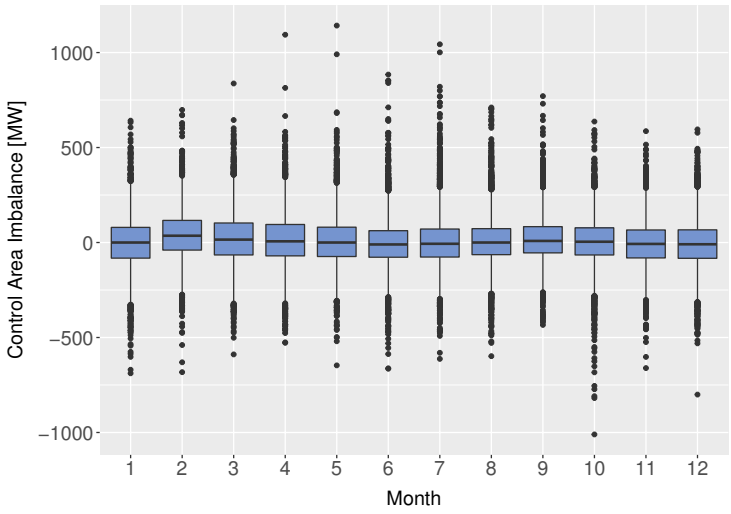

Figure 4.2: Control area imbalance during the years 2015 - 2020. Boxplots grouped per month. Mostly similar extends of whiskers can be observed, with medians slightly differing around 0 MW.

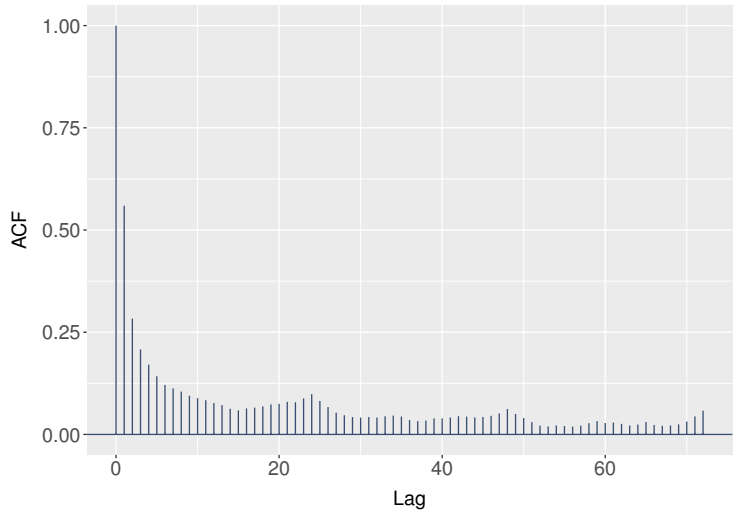

Figure 4.3: Autocorrelation, with lag in hours: Control area imbalance during the years 2015 - 2020. The autocorrelation drops fast during the first three days with visible peaks for full days (lag 24, 48 and 72).

4.3 Electricity Market: Important Variables

There are various variables that have an impact on fluctuations in consumption and generation of electricity and can thus also influence the demand of balancing energy. From now on forecast errors always describe the difference between day ahead forecasts and realized values (regarding load or generation) on the day of delivery. The following variables are considered for further analysis:

- Load - level, forecast, forecast error
- Day ahead price
- Feed-in from Solar - realized value, forecast, forecast error
- Feed-in from Wind - realized value, forecast, forecast error

Day ahead prices are available after the market clearing and can be retrieved from the EPEX. They are usually available at 12:00 (CET+1), but can be delayed by a few minutes on some days. Load as well as solar- and wind-generation forecasts are published on the ENTSO-E transparency platform[1] no later than 18:00 (CET+1) for the entirety of the following day ("day ahead forecast").

[1] `https://transparency.entsoe.eu/`

This entails, that with the latter publication all used data is published and the predictions for the control area imbalance can be made.

4.3.1 Load

Load describes the total consumption of electricity. When forecast errors occur, this leads to an increase or a decrease in electricity feed in to ensure the operation of a balanced network. A sharp rise or fall of the load can lead to adjustment difficulties concerning the producers, which can result in a need for balancing energy. It should be noted that the design of the electricity market, in particular the discrete billing intervals of the balancing groups respectively the trading of hourly products on the electricity market, can lead to sudden deviations in the electricity grid. Even if the forecast of demand of electricity in a specific time interval (made from the balancing group) is correct, nevertheless often they do not make (short-term) adjustments[2] and that can lead to short-term surpluses or deficits [Maurer, 2010]. This is shown in figure 4.4.

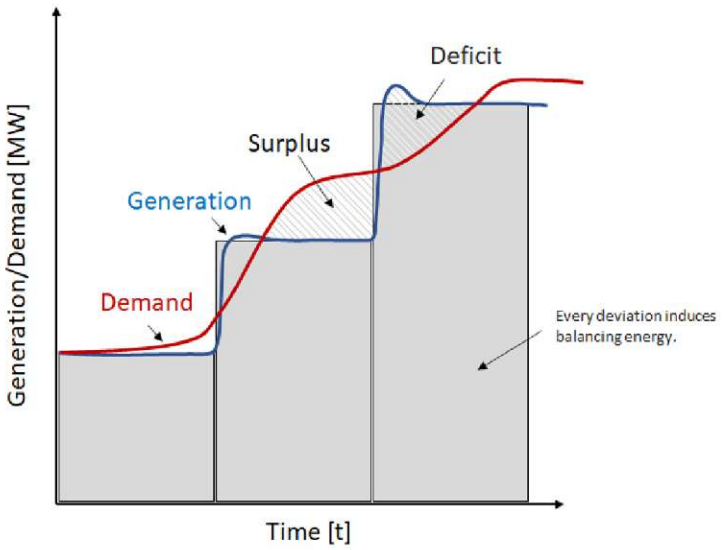

Figure 4.4: Difficulties in an electricity market with hourly products: Due to the blockwise (time periods) resolution of traded products, mismatches between demand - that follows a continuous path - and generation can occur even for perfect forecasts.

[2] Consider for example a small - but commercial - consumer that fails to update its balancing group leader of any (short-term) changes in consumption (e.g. employees starting up or shutting down big machinery).

Figure 4.5 describes the average load within Austria in the years 2015 to 2020. It can be seen that the average load has remained relatively the same over the last five years. However, a small decline can be seen in 2020. This decline can be explained by the measures taken to contain COVID-19. These had a significant impact on electricity consumption in Austria. In some cases, the weekly requirement fell by around ten percent compared to normal consumption [Statista, 2020].

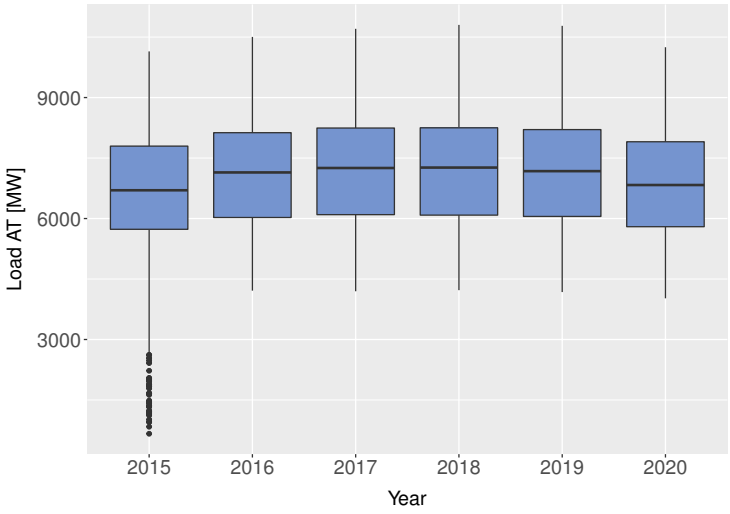

Figure 4.5: Boxplots: Realized load in Austria for each year from 2015 - 2020. Only small shifts of the yearly median can be observed, but the years 2019 and 2020 showcase that electricity demand does not steadily increase each year.

Figure 4.6 shows the average load in Austria for each hour from 2015 to 2020. The difference between "peak" (8:00 a.m. to 8:00 p.m.) and "off-peak" (0:00 a.m. to 8:00 a.m. and 8:00 p.m. to midnight) hours can clearly be seen.

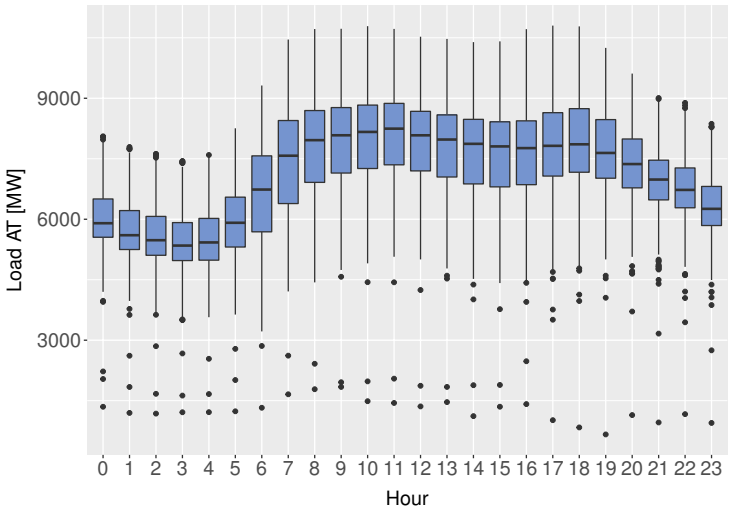

Figure 4.6: Boxplots: Realized load in Austria during the years 2015 - 2020, grouped per hour. A daily pattern can be observed, with low demand during night time ("offpeak") and comparably higher demand during the day ("peak"). Only a few outliers can be observed, but most hours showcase large deviations, with demand during the day ranging between 4500 and 10500 MW.

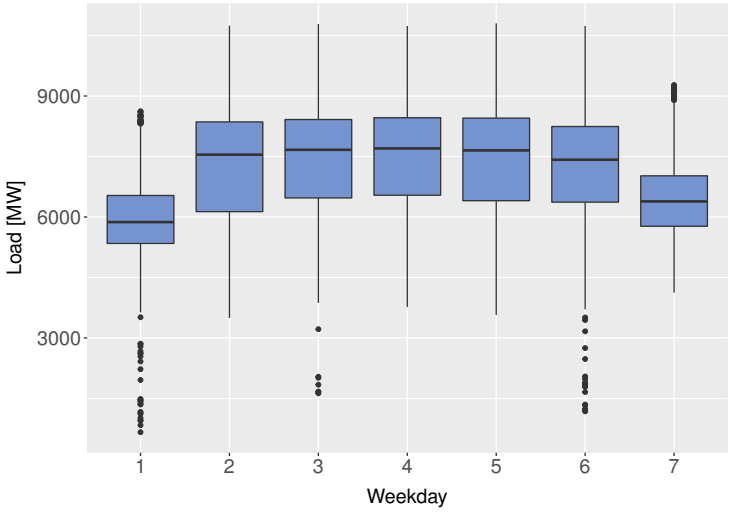

Figure 4.7: Boxplots: Realized load in Austria during the years 2015 - 2020, grouped per weekday (starting the week with Sunday="1"). A clear pattern can be observed with load dropping significantly on weekends. More outliers in loads can be observed on Fridays and Sundays.

Originally, load forecast errors were considered based on the hourly average for 2015 to 2020. This showed clear differences between individual hours: the forecast error in the off-peak hours is positive on average and has negative values in the peak hours. However, there are big differences between the individual years. Therefore, figure 4.8 shows the forecast error grouped per year. The median forecast error per year from 2015 to 2017 is negative. A positive median forecast error per year can be seen in the years 2018 to 2020. As explained in 2.3 in May 2017, the German and Austrian regulatory authorities (BNetzA and E-Control) agreed to separate the common electricity price zone. The separation of the Germany-Austria electricity price zone came into effect on October 1, 2018. The separation of the price zones led to a restructuring of the market.
To investigate the effect of events like that, structural breaks in given data can be examined with the help of statistical tests. In 4.4, amongst other things, the Chow-Test will be used to investigate structural breaks.

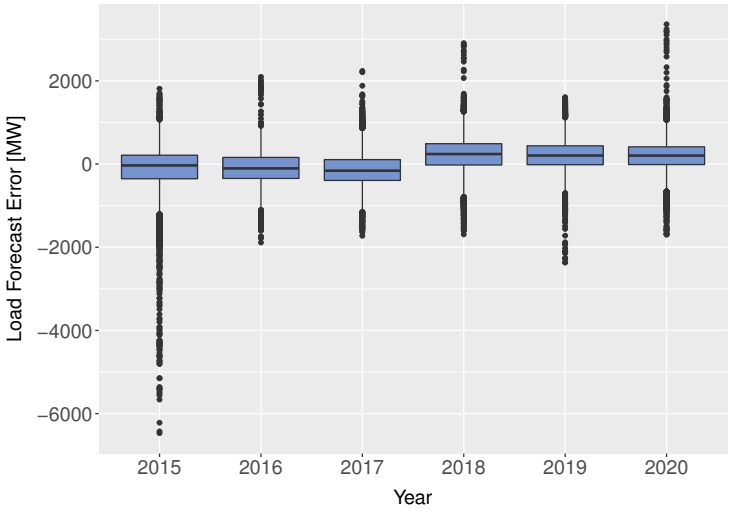

Figure 4.8: Load forecast error during the years 2015 - 2020. Separate boxplots for each year. Relatively small "boxes" (covering the range from the first to the third quantile), but many outliers, can be observed. The medians shifting from negative to positive show a large shift of errors comparing the years (2015, 2016, 2017) against (2018, 2019, 2020).

Figure 4.9 shows the QQ-plot of the load forecast error versus the quantiles of a normal distribution. About 50% of the load forecast error is between $\pm$ 280 MW. When considering the autocorrelation with a maximum lag of 72 hours (three

days) a slow decrease in correlation can be seen. The autocorrelation over the period of a whole year almost approaches zero. Here, the lag of 72 hours was considered to ensure consistency with the other figures that show an autocorrelation.

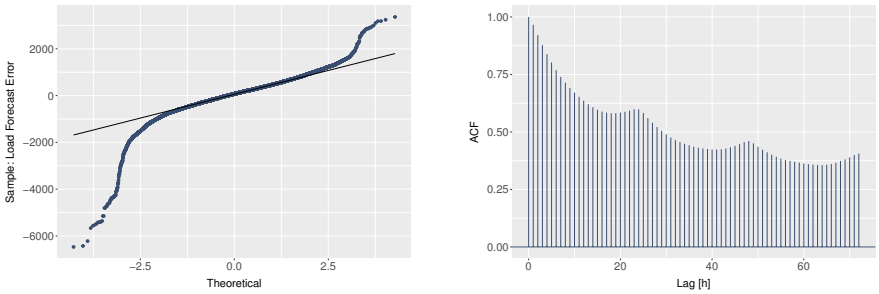

Figure 4.9: The left plot compares the theoretical quantiles of a normal distribution against the quantiles of the load forecast error and reveals large deviations. The right plot highlights that the autocorrelation of load forecast errors only drops slowly, with visible peaks for whole days (24, 48 and 72 hours). This could hint at "systematic errors" that are repeated over a longer period of time and either continuously over- or underestimate the load.

In figure 4.10 two different scatter plots are shown. In 4.10a the absolute load forecast error $|FCE_{Load}|$ versus the load forecast FC_{Load} is plotted. In 4.10b the load forecast error FCE_{Load} versus the load forecast FC_{Load} is plotted.

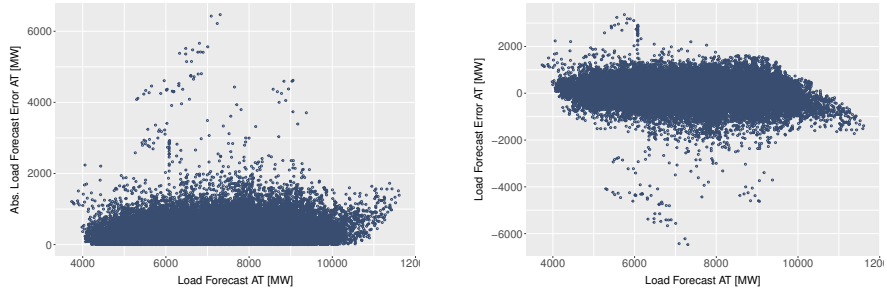

(a) $|FCE_{Load}|$ vs. FC_{Load} (b) FCE_{Load} vs. FC_{Load}

Figure 4.10: Plotting load forecast error (absolute values used for the left plot) over the load forecast during the years 2015 - 2020 reveals no clearly visible patterns. It can however be observed that the absolute error seems to increase with the forecast starting at 10000 MW, while the right plot suggests that positive forecast errors get more unlikely the higher the forecast gets.

4.3.2 Day Ahead Prices

As already explained in 2.4.1 the term day ahead trading refers to the trading of electricity for the following day, which takes place mostly on the EPEX Spot in Paris. In the German and Austrian markets, the bids for the auctions for the next day must be submitted by noon. The results of the corresponding surcharges are published at 12:40 p.m. each day [Kraftwerke, 2020]. Figure 4.11 shows the boxplots of the day ahead prices grouped per hour from 2015 to 2020. It can be clearly seen that in hours 21 to 6 the prices are on average significantly cheaper than in hours 7 to 20, Although, a fluctuation around noon can be seen.

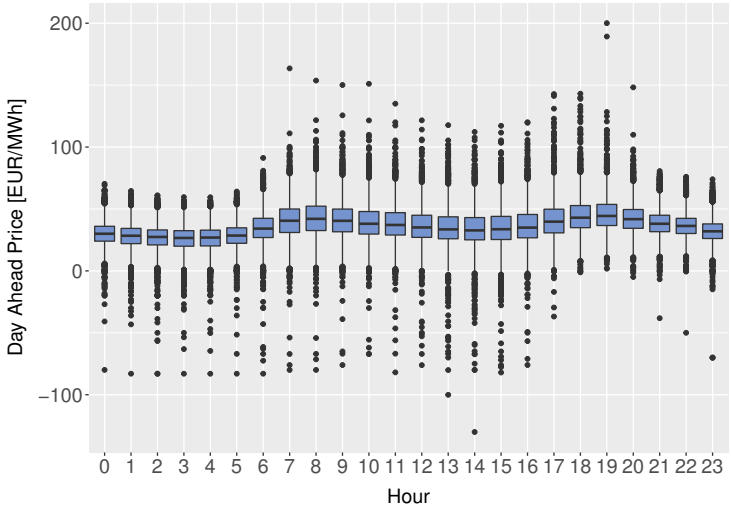

Figure 4.11: Day ahead price during the years 2015 - 2020, with separate boxplots per hour. A daily pattern - similar to the plot regarding the hourly electricity demand - can be observed, featuring slightly lower median prices during nighttime hours.

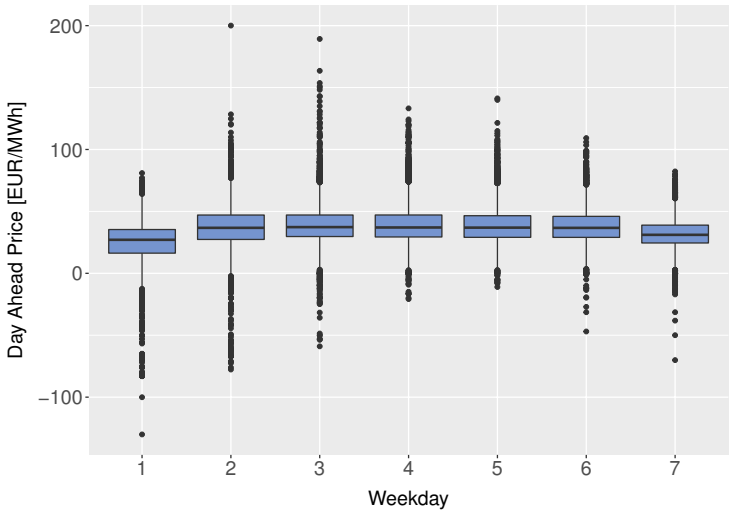

Figure 4.12: Day ahead price during the years 2015 - 2020, with separate boxplots per weekday ("1" = Sunday). A small decrease of prices during weekends - possibly linked to a lower overall demand - can be observed, while prices from Monday-Friday depict a similar course.

4.3.3 Renewable Energies

The feed in to the electricity grid through wind and solar is an important emission-free and future-oriented source of energy. However, wind and solar plants are not under perfect control of humans and are subject to the laws of nature, which leads to possible forecast errors on the supply side. It should be noted that times with very high and very low feed-in by wind and solar can usually be predicted better than times with medium feed-in [Jost et al., 2015b]. Data on solar and wind energy from 2015 to 2020 in Austria is analyzed. As already mentioned in 2.1 the expansion of renewable energies, especially solar and wind energy, is making steady progress in Austria. Figure 4.13b shows a continuous increase in solar energy generation from 2015 to 2018, with a small decrease for 2019 and 2020. This increase in generation can be explained by an additional installed capacity of 1128 MW, compared to the end of 2015, resulting in a total installed capacity of 1851 MW in 2021 [APG, 2020]. The situation is similar with wind energy. Figure 4.13a shows an increase in wind energy generation from 2015 to 2020. This increase in generation can be explained by an additional installed capacity of 701 MW, compared to the end of 2015, resulting in a total installed capacity of 3198 MW in 2021 [APG, 2020].

The highest level of electricity generation from wind energy was achieved in 2019, while a decline in production in 2020 can also be seen.

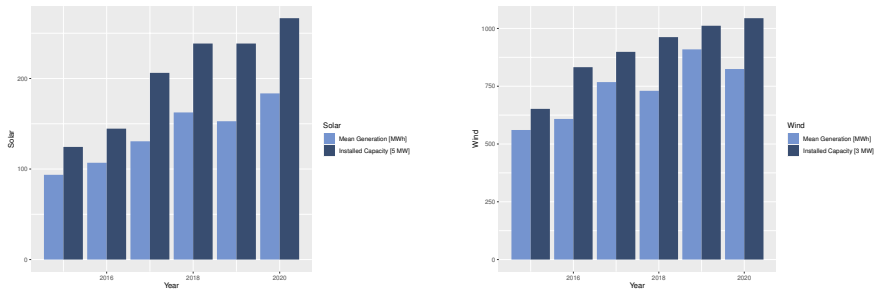

(a) Solar (b) Wind

Figure 4.13: Average hourly generation and installed capacities for wind and solar during the years 2015 - 2020 [APG, 2020]. While the installed capacities continuously rise, it can be observed that this does not always result in increased amounts of energy being generated, since those also depend on weather-based availability.

The generation of solar energy in Austria from 2015 to 2020 is considered in figure 4.14. As expected in 4.14a a clear daily seasonality can be seen, which results from the hours of sunshine per day. Strong monthly seasonality can also be recognized in 4.14b. Timestamps of all available data are given respecting the Austrian local time. This entails that winter and summer hours are not exactly the same (since their UTC differs), but better depicts time-dependent variables. To keep data consistent these timestamps are used for all variables.

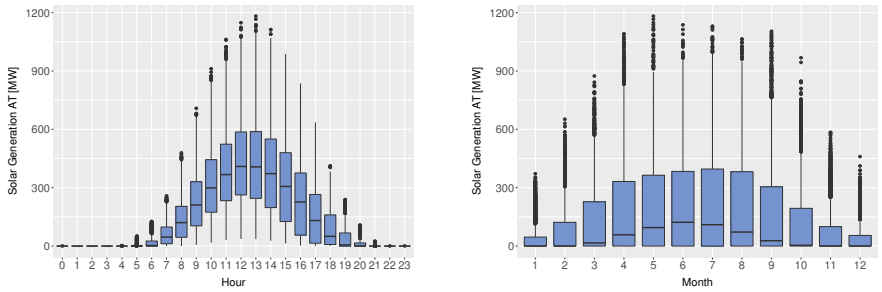

(a) Grouped per hour (b) Grouped per month

Figure 4.14: Solar generation in Austria during the years 2015 - 2020 grouped per hour (left) and month (right). Both plots show clear patterns, favoring high generation during midday and summer-times, but also show that the generation during "offtimes" (like during mornings or non-summer months) can sometimes exceed generation during more favorable times.

Particularly when viewed monthly (showed in 4.15b), a clear seasonality can be seen in wind energy generation. Especially in the months from June to September, the median generation from wind energy is relatively low compared to the rest of the year. Looking at the generation of wind energy grouped per hour in 4.15a, it can be observed that wind generation accounts for around 10% of the Austrian load.

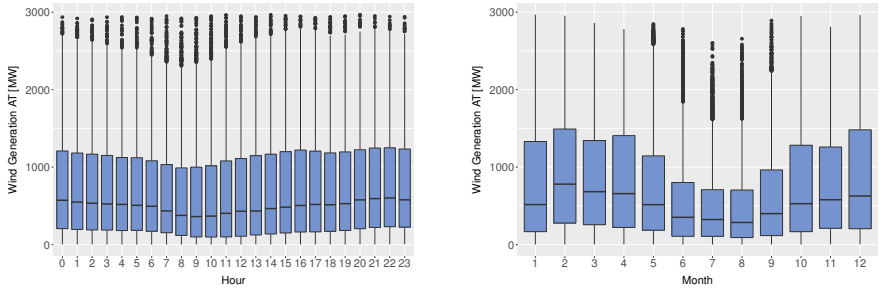

(a) Grouped per hour (b) Grouped per month

Figure 4.15: Wind generation in Austria during the years 2015 - 2020 grouped per hour (left) and month (right). Both plots showcase a much more stable generational profile than solar, but also highlight an inverse relationship with wind generation dropping slightly during hours and months were solar generation peaks.

The histogram in figure 4.16 of the solar and wind generation in Austria from 2015 to 2020 shows that about 50% of the solar generation per hour is smaller

than 15.75 MW (this low value is due to the fact that no solar energy generation is possible at night) and about 50% of the wind generation per hour is smaller than 495 MW.

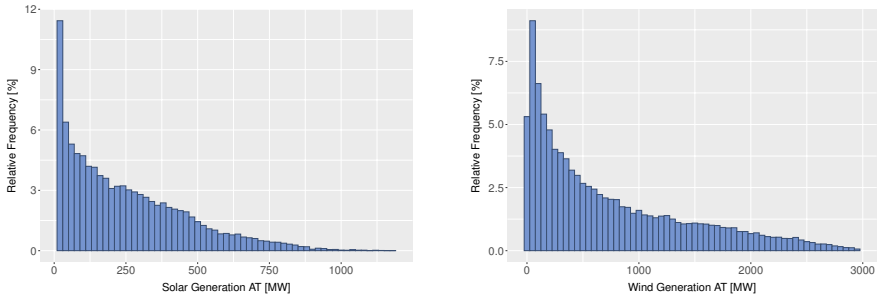

(a) Solar (b) Wind

Figure 4.16: Histogram: Renewable energy generation for wind and solar during the years 2015 - 2020. Both plots show that lower generation values are more likely for both technologies.

In the following, the forecast error of renewable energies (wind and solar) is considered. The figure 4.17 shows a QQ-plot and a scatter plot. In the QQ-plot the solar forecast error versus the quantiles of the normal distribution as well as the wind forecast error versus the quantiles of the normal distribution is plotted. In scatter plot 4.17a the relatively good forecast quality for solar energy can be seen. The scatter plot in 4.17b shows that the wind forecast quality cannot match that of the solar forecast quality.

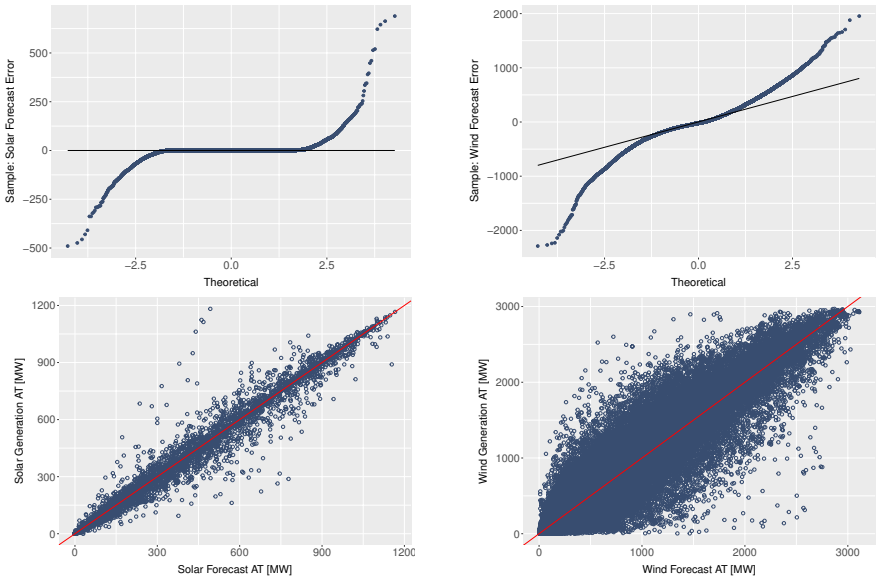

(a) Solar (b) Wind

Figure 4.17: QQ-plots and scatterplots for renewable energy forecast errors during the years 2015 - 2020. The plots show a superior quality of solar forecasts compared to wind forecasts. It shall here be noted, that the minimum reported resolution of measurements of 1 MW favors the much lower values (due to less installed capacity) of solar, generating much more "perfect" (forecast error equal to zero) forecasts. This excess of solar forecast errors being zero can be observed in the mostly horizontal QQ-plot of the solar forecast error.

In figure 4.18 two different scatter plots are shown. In 4.18a the absolute solar forecast error $|FCE_{Solar}|$ versus the solar forecast FC_{Solar} is plotted. In 4.18b the solar forecast error FCE_{Solar} versus the solar forecast FC_{Solar} is plotted.

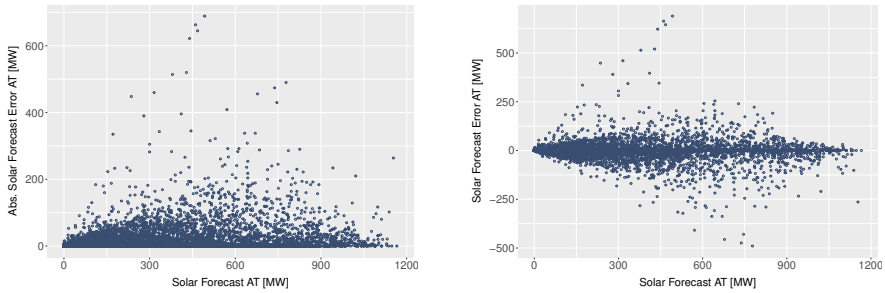

(a) $|FCE_{Solar}|$ (b) FCE_{Solar}

Figure 4.18: Solar forecast error (absolute values in the left plot) plotted over the solar forecast during the years 2015 - 2020 showing no obvious patterns.

In figure 4.19 two different scatter plots are shown. In 4.19a the absolute wind forecast error $|FCE_{Wind}|$ versus the wind forecast FC_{Wind} is plotted. In 4.19b the wind forecast error FCE_{Wind} versus the wind forecast FC_{Wind} is plotted.

(a) $|FCE_{Wind}|$ (b) FCE_{Wind}

Figure 4.19: Wind forecast error (absolute values in the left plot) plotted over the wind forecast during the years 2015 - 2020. The supposedly observable pattern in the right plot is only created by definition of $FCE = actual - forecast$ and hours were no generation was realized.

Figure 4.20 shows the autocorrelation for the solar and wind forecast error. In this figure a lag with 72 hours (three days) is chosen. A strong decrease in the correlation can be seen as, it almost approaches zero for the forecast error of solar and wind energy.

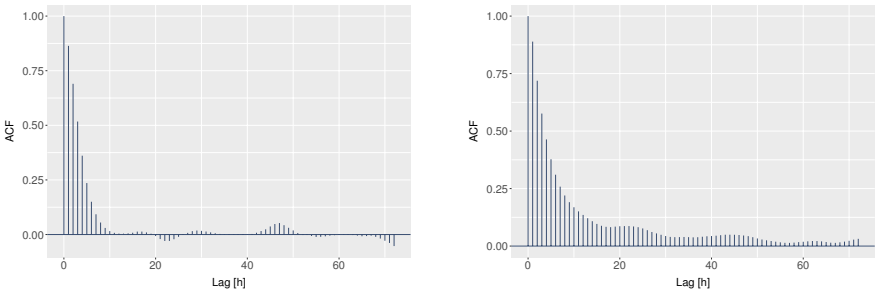

(a) Solar (b) Wind

Figure 4.20: Autocorrelation: Forecast errors of wind and solar during the years 2015 - 2020. Besides small peaks for lags of whole days, it can be observed that wind forecast errors propagate more into the future with an autocorrelation that drops much slower.

4.4 Structural Breaks

The previous consideration of the data suggests that there exist structural breaks in the considered time period. The Chow-Test is one possibility to verify structural breaks.

4.4.1 Chow-Test

A data record with the form (y_i, x_i) is given , whereby the relationship between the variables is described by a linear function with a normally distributed error with an expected value of 0. The assumption is made that the dataset can be divided into two groups of size N_a and N_b that are better described by two different linear functions:

$$y_i = \beta_0 + \beta_1 x_{i1} + \beta_2 x_{i2} + ... + \beta_k x_{ik} + u_i \text{ with } i \in [1, N_a]$$
$$y_i = \alpha_0 + \alpha_1 x_{i1} + \alpha_2 x_{i2} + ... + \alpha_k x_{ik} + u_i \text{ with } i \in [N_a + 1, N_a + N_b]$$

It follows that $N = N_a + N_b$ and the null hypothesis $H_0 : (\beta_0, \beta_1, ..., \beta_k) = (\alpha_0, \alpha_1, ..., \alpha_k)$ is tested against the alternative hypotheses $H_1 : (\beta_0, \beta_1, ..., \beta_k) \neq (\alpha_0, \alpha_1, ..., \alpha_k)$.
If one denotes the sum of the squared residuals of the regression over the entire dataset with S and over the two subgroups with S_a and S_b, then the defined test variable T follows an F-distribution with $f_1 = k+1$ and $f_2 = N_a + N_b - 2(k+1)$ degrees of freedom. T is defined as follows:

$$T := \frac{(S-(S_a+S_b))/(k+1)}{(S_a+S_b)/(N_a+N_b-2(k+1))}$$

If $T \geq F_{f_1,f_2,1-\alpha}$ (level of significance $\alpha = 0.05$) then the null hypothesis H_0 can be rejected. This means that the two regression lines on the sub-intervals are not identical and there is evidence that a structural break could potentially exist and that the partial regressions would therefore provide better modeling than a regression over the entire dataset.

4.4.2 Breakpoints

Many applications make it reasonable to assume that there are a n breakpoints (instead of only a single one), where the coefficients change from one stable regression relationship to another one. This implies, that there are $n + 1$ "separable" segments in which the regression coefficients remain constant. The STRUCCHANGE package [Hurtado, 2020] in *R* [R Core Team, 2013] enables testing/searching for these breakpoints in an automated fashion, based on a dynamic programming approach. Furthermore the corresponding breakpoints (the timestamps that best separate the $n + 1$ segments) are reported.

4.4.3 Results

All variables were examined for structural breaks using the Chow-Test explained in 4.4.1. It is important to note however, that a "positive" result of the Chow-Test does not immediately imply a hard structural break, it is merely one of many possible hints that a break could exist. Changes in regression coefficients (indicated by the Chow-Test) could for example also be caused by newly installed capacity (changing the total generation values). Furthermore, the *breakpoints* function was used to estimate optimal structural breaks. Both approaches are explained in more detail below.

Approach

All Chow-Tests (using a regression on the intercept β_0) were done in *R* [R Core Team, 2013] using *sctest* from the STRUCCHANGE package [Zeileis et al., 2019]. The single timestamp that was used to test for a structural break is "October 1, 2018" (date of the price zone separation of Austria and Germany). Estimating optimal structural breaks was implemented in *R* [R Core Team, 2013] using *breakpoints* from the STRUCCHANGE package [Hurtado, 2020]. This allows the possibility to search for an arbitrary number (here $k = 5$) of structural breaks in the whole data. Since the overall data was too large to handle (and *breakpoints* could not be applied in a reasonable amount of time), first the hourly data was summarized into daily data (using the daily mean).

This results in a timeseries with 2193 days that was then analyzed for every variable of interest. Since *breakpoints* does not return p-values, all reported dates where again checked with a Chow-Test, which resulted in p-values close to zero, indicating a significant structural break at or near these dates.
The following sections document the results for both approaches for every variable.

Load Forecast Error

As already seen, in figure 4.8 suggests a structural break at the time of the price zone separation of Austria and Germany.
The Chow-Test provides the following result:

$$T = 4841.3 \text{ and } p - value < 2.2 \cdot 10^{-16}$$

This means that the null hypothesis H_0 is rejected and so it is highly likely that there is a structural break on October 1, 2018.

The function *breakpoints* hints at a total of four possible structural breaks with the most dominant found on April 24, 2018. Comparing the first and second time-period (January 1, 2015 to April 24, 2018 and April 24, 2018 to December 31, 2020) one can observe a mean of -117 MW and 187 MW respectively. This showcases the big difference between the load forecast errors in each interval. The standard deviation in the two periods shows only a minor difference: 407 MW and 387 MW.

Solar Forecast Error

The Chow-Test provides the following result:

$$T = 21.034 \text{ and } p - value < 5 \cdot 10^{-6}$$

This means that the null hypothesis H_0 is rejected and so it is highly likely that there is a structural break on October 1, 2018.

Estimating optimal breakpoints using *breakpoints* fails to find any breakpoints.

Wind Forecast Error

The Chow-Test provides the following result:

$$T = 298.64 \text{ and } p - value < 2.2 \cdot 10^{-16}$$

This means that the null hypothesis H_0 is rejected and so there is a structural break on October 1, 2018.

The function *breakpoints* hints at a total of three possible structural breaks with the most dominant found on October 6, 2018. Comparing the first and second time-period (January 1, 2015 to October 6, 2018 and October 6, 2018 to December 31, 2020) one can observe a mean of 47 MW and 209 MW respectively. This showcases the big difference between the wind forecast errors in each interval. The standard deviation in the two periods shows only a minor difference: 257 MW and 287 MW.

Day Ahead Price

The Chow-Test provides the following result:

$$T = 1460.5 \text{ and } p - value < 2.2 \cdot 10^{-16}$$

This means that the null hypothesis H_0 is rejected and so there is a structural break on October 1, 2018.

The function *breakpoints* hints at a total of four possible structural breaks with the most dominant found on May 20, 2018. Comparing the first and second time-period (January 1, 2015 to May 20, 2018 and May 20, 2018 to December 31, 2020) one can observe a mean of 26 EUR and 41 EUR respectively. This showcases the big difference between the day ahead prices in each interval. The standard deviation in the two periods shows only a minor difference: 9 EUR and 13 EUR.

Control Area Imbalance

The Chow-Test provides the following result:

$$T = 0.89913 \text{ and } p - value = 0.343$$

This means that the null hypothesis H_0 can not be rejected and so no further conclusion about a structural break on October 1, 2018 can be drawn.

The function *breakpoints* hints at a total of three possible structural breaks, with none of them being later than 2017. This indicates no systematic changes of the outcome variable CAI during the period (2019 and 2020) that is later on analyzed.

4.5 Conclusion

Generation of solar and wind energy has increased throughout the years, partly due to the expansion of the respective power plants. While the generation of electricity by solar energy is clearly dependent on the time of day or the month, generation by wind energy is relatively independent of the time of day (slight decline between 8 a.m. to 11 a.m.), but a decline in generation occurs in the months of July to September. It can also be seen that the forecast of solar energy is significantly better than that of wind energy.
A structural break analysis was carried out using a Chow-Test and the optimal breakpoints where estimated using *R* [R Core Team, 2013]. The Chow Test hints at significant structural breaks during 2018 for all variables except the control area imbalance. These structural breaks are, among other things, possibly the result of the price zone separation of Austria and Germany at October 1, 2018. The expansion of renewable energies can be identified as a further influencing factor.

In addition, the representation of the autocorrelation of the operational data of the control area imbalance (2015 to 2020) suggests a weak autocorrelation (shown in figure 4.3). Analyzing the control area imbalance - that will be used as final outcome variable in the following proposed model - revealed no extreme differences comparing values grouped per months, weekdays or hours. Furthermore, the Chow-Test did not indicate a structural change during the separation of price zones, as well as no potential breakpoints were found starting from 2018. This hints at a rather stable course of the timeseries and no systematic changes, which plays an important role when modelling and explaining the control area imbalance.

Since the analysis hints at many structural breaks and changes during or leading up to 2018, the data from 2019 and 2020 will be used in the following sections to build the model.

Chapter 5

The Model

The main goal presented in this thesis is a day ahead forecast of the control area imbalance. Therefore input data that is available at the time of the forecast (day ahead) from 2019 and 2020 (with a focus on renewable energies) is used. The model is split into two stages. In stage I the absolute forecast error of load, solar and wind is analyzed using different mathematical methods. The result of stage I is then used as additional input for stage II, in which the absolute control area imbalance is predicted.

5.1 Stage I - Forecast Errors

In stage I of the model three mathematical methods (multiple linear regression, tobit model and quantile regression) are considered in order to analyze the absolute value of the load, wind and solar forecast errors.
The following section gives a complete overview about the mathematical models that are used, including all explanatory variables. Later on some insight into different ways of estimating the unknown coefficients are presented and the chapter concludes with an in-depth analysis of model results and compares the outcomes using the MAE and RMSE.

5.1.1 Mathematical Model

First of all the mathematical model that is used in stage I is defined. For this the definition of the absolute forecast error is needed. In this thesis the absolute forecast error is calculated as the absolute value of the difference of the actual

output (actual load, actual wind generation or actual solar generation) and the forecast (load, wind or solar forecast).
Due to the assumption that current, available forecasts are already reasonably good it is highly unlikely to correctly estimate the forecast error. This would entail that the current forecast could be improved using historic values of the same timeseries and publicly available (aggregated) data for demand and generation; a fact that would contradict the initial assumption.
This however does not imply that estimating the absolute deviation from the expected value (which is always zero for the control area imbalance since otherwise the control area would not be balanced by design) is impossible. Since it can be seen that the absolute quantity of mismatch between expected load/generation and actually realized load/generation plays an important role and influences the power market and grid, the absolute forecast errors will be considered from now on.
In the following, three absolute forecast errors are considered as endogenous variables y_i with $i \in \{Load, Solar, Wind\}$:

1. Absolute Load Forecast Error ($|FCE_{Load}|$)
2. Absolute Solar (Generation) Forecast Error ($|FCE_{Solar}|$)
3. Absolute Wind (Generation) Forecast Error ($|FCE_{Wind}|$)

The mathematical model is intended to describe the three endogenous variables (absolute load, solar and wind forecast errors) by exogenous variables that are used below. The chosen explanatory variables were selected based on the results from Chapter 4.
The descriptive analysis showed, sometimes high, autocorrelation of the various forecast errors, with all of them showcasing a small peak at the lag of 24 - which represents the same hour of the day as yesterday. Since it is assumed that the day ahead forecast is made at the end of each day (using all available data) for the following day, the realized forecast errors of the current day are already known and can be used as predictive factors.
It could be expected, that the magnitude of the forecast plays an important role in the to-be-realized forecast error. This is due to the fact that forecasts of different magnitudes can result in an increased or decreased volatility (meaning that for example the wind forecast gets worse the higher the forecast amount of wind is). Since it is not known whether this relation is strictly linear or behaves in a non linear way (it could for example happen that really high forecast introduce a much higher error term than what would be explained by a linear

term or vice versa) the squared forecast is also included. The results in table 5.4, 5.5 and 5.6 show that this in fact is true.
The solar forecast FC_{Solar} is used in all models as proxy to estimate the current weather situation: Since weather data could influence the wind generation (e.g. possible curtailment in stormy weather) and load (e.g. increased demand for electricity due to air condition, decreased private demand in times of "good weather", ...) it could be important to include this in a regression model. Since unfortunately hourly exact weather data was not available for this thesis, the solar forecast (as indicator of solar irradiance) is used.
All three endogenous variables showcase noticeable differences during different hours of the day and month of the year. While the load depicts the "usual" course during peak/offpeak hours, solar generation is (as expected) highest during midday hours, while wind showcases the opposite course with lower generation during the daytime. This inverse relationship also holds true for the monthly values with solar generation peeking in mid summer, while wind generation drops from close to 1000 MW (on average during 2015-2020) during winter months to less than 500 MW in July and August.
The generation of solar and wind energy is independent of the day of the week. If differences in generation arise throughout the week, they are connected to differences in the electricity demand between weekdays and weekends or other market effects. This is the reason that the weekday as exogenous variable was only added to the model of the load.
As it is often used, binary dummy variables are introduced to describe the influence of single hours, weekdays or months. For all periods these dummy variables are defined similar to the hourly ones (assuming the input variable $hour \in \{1, \dots, 24\}$:

$$hour_h = \begin{cases} 1, & \text{if } hour = h \\ 0, & \text{otherwise} \end{cases}$$

Since it is not clear at this point, whether the day ahead price has any influence on the forecast errors, it is taken into account in all three models and its significance is evaluated later on, based on the results of the different regression models. Table 5.4, 5.5 and 5.6 again show that the inclusion of the day ahead price makes sense. Although, the quantile regression views it as sometimes not significant (as can be seen in the mentioned tables).
The following section write out the chosen models in full detail. Abbreviations used are explained in table 5.1.

Table 5.1: Abbreviations - Stage I

Abbreviation	Description
FC_i	Forecast of various variables: $i \in \{Load, Solar, Wind\}$
FCE_i	Forecast error of various variables: $i \in \{Load, Solar, Wind\}$
$FCE_{i,day-1}$	Lagged forecast error of various variables $i \in \{Load, Solar, Wind\}$. This uses the forecast error that occured on the previous day during the same hour (therefore "$day-1$").
$price_{DA}$	Day ahead price published on EPEX Spot
$hour$	Hour of the day
$hour_h$	$hour_h = 1$ if $hour = h$, 0 otherwise
$month$	Month of the year
$month_h$	$month_h = 1$ if $month = h$, 0 otherwise
$wday_d$	$wday_d = 1$ if the day of the week is d, 0 otherwise
u	Residuals

Load

The chosen model for the absolute load forecast error is as follows:

$$\begin{aligned} |FCE_{Load}| = \; & \beta_0 + \beta_1 \cdot FC_{Load} + \beta_2 \cdot |FCE_{Load,day-1}| \\ & + \beta_3 \cdot price_{DA} + \beta_4 \cdot FC_{Solar} \\ & + \sum_{h=1}^{24} \beta_{5,h} \cdot hour_h + \sum_{m=1}^{12} \beta_{6,m} \cdot month_m \\ & + \sum_{d=1}^{7} \beta_{7,d} \cdot wday_d + u \end{aligned} \tag{5.1}$$

Solar

The chosen model for the absolute solar forecast error is as follows:

$$\begin{aligned} |FCE_{Solar}| = \; & \beta_0 + \beta_1 \cdot FC_{Solar} + \beta_2 \cdot FC_{Solar}^2 \\ & + \beta_3 \cdot |FCE_{Solar,day-1}| + \beta_4 \cdot price_{DA} + \beta_5 \cdot hour \\ & + \beta_6 \cdot hour^2 + \beta_7 \cdot month + \beta_8 \cdot month^2 + u \end{aligned} \tag{5.2}$$

Wind

The chosen model for the absolute wind forecast error is as follows:

$$\begin{aligned} |FCE_{Wind}| = \ & \beta_0 + \beta_1 \cdot FC_{Wind} + \beta_2 \cdot |FCE_{Wind,day-1}| \\ & + \beta_3 \cdot price_{DA} + \beta_4 \cdot FC_{Solar} \\ & + \sum_{h=1}^{24} \beta_{5,h} \cdot hour_h + \sum_{m=1}^{12} \beta_{6,m} \cdot month_m + u \end{aligned} \tag{5.3}$$

As an explanation why the models showcase some small differences:

Difficulties estimating Variance-Covariance

It shall be noted here, that all measured variables (load, solar and wind generation) are measured with an accuracy of 1 MW. This obviously results in forecast errors being exactly zero more often than it would happen if "exact" measurements would be available.
When choosing the previously mentioned explanatory variables for all three models (absolute load, solar and wind forecast error), using the three mathematical methods explained below in section 5.1.2, multiple difficulties arise which are all closely related to inverting a poorly conditioned matrix during the process of determining all coefficients, their standard errors and significance.
First, the tobit model for the absolute load forecast error returns an error while calculating all results. The same error occurs (for a different reason) in the tobit parameter estimation of the absolute solar forecast error: Using all described exogenous variables leads to the matrix $X'X$ being almost singular (with X indicating the regressor matrix). This prevents the algorithm from inverting said matrix, which is needed to calculate the estimators for all parameters (the coefficients β and variances σ).
The exact reason can not be fully determined since the used algorithms in R only terminate with a general error message, that does not contain any further detailed information. Nevertheless, it can be guessed that this is closely related to a strong correlation between the load and load^2 terms, since the removal of the squared term fixes the problem. Due to this the quadratic load term was removed from all models. It was later on decided to not include the results of the tobit model for the absolute wind and load forecast error in this thesis (since they are indistinguishable from the results of the multiple linear regression), but the model structure was kept in place like explained.

The reasoning in the solar model is different: Due to the fact, that times of "sun - availability" vary throughout the year, it happens that some combinations of explanatory variables are underrepresented in the dataset. For example, during the winter months, late hours (after 16:00) with a positive solar generation are becoming less likely with some combinations of month/hour only occurring a few times. This again leads to singular Hessian matrix, which - in this case - can be fixed by using the original continuous variable instead of binary dummies. In order to roughly estimate the daily/hourly pattern of different influential factors (e.g. solar irradiance), the monthly and hourly (continuous) terms are also added as squared term.
The difficulties explained in the previous paragraphs can be investigated by looking at the regressor matrix X, more precisely comparing the condition number of $X'X$ (since that is the matrix that is inverted during the calculation of the estimators for all parameters - the coefficients β and variances σ). The condition number of a matrix is a measure how close it is to being singular (and therefore not invertible), with a condition number of 1 for "far away from singular" up to ∞ for a singular matrix. This entails that the lower the condition number is, the better (for this case). Table 5.2 shows that removing the squared load forecast from the load model and respectively the time-based dummy variables (hour, month and weekday) from the load model reduces the condition number of $X'X$ in both models by a considerable amount. It should however be noted, that both matrices are still poorly conditioned, with condition numbers greater than 10^7.

Table 5.2: Condition numbers of $X'X$ for the load and solar model, indicating "how close to being singular" the matrix is. It can be seen that the proposed simple changes reduce the condition number by a great magnitude.

Model	Condition number	Note
Load	$4 \cdot 10^{18}$	Complete model
Load	$9 \cdot 10^{10}$	Load model without squared forecast
Solar	$8 \cdot 10^{13}$	Complete model
Solar	$6 \cdot 10^{7}$	Solar model without squared forecast and with continuous time-variables instead of ordinal / factor-based variables.

5.1.2 Estimating coefficients

The mathematical models that will be analyzed in more detail using a multiple linear regression, a tobit model and a quantile regression are already defined. These different methods of analyzing the mathematical model, as well as their

implementation in *R* [R Core Team, 2013] are explained in theory below.

Multiple Linear Regression

Regression analysis is a statistical technique used to analyze the relationship between several variables. Specifically, it is about explaining a variable using a function of other variables. The variable to be explained is called the dependent variable or endogenous variable. The variables used for clarification are the so-called independent or exogenous variables. Often these independent variables are also called regressor variables or regressors. These are mathematically written as

$y_t \in \mathbb{R}$ with $t = 1, ..., T$	Observations of the dependent (endogenous) variable y
$x_{tk} \in \mathbb{R}$ with $t = 1, ..., T, k = 1, ..., K$	Observations of the independent (exogenous) variables x_k

The aim is to approximate the dependent variable y using a function of the independent variable x_k:

$$y = x_1\beta_1 + ... + x_K\beta_K + u$$

The unknown parameters β_k are to be determined in such a way that the residuals $u = y - (x_1\beta_1 + ... + x_K\beta_K)$ are as small as possible [Scherrer, 2015].

The unknown parameter vector is estimated on the basis of a sample. For this there exist different procedures, the best known in this context is the Ordinary Least Squares estimation (OLS). The non explainable differences that are resulting from an estimation procedure are called residuals u. The OLS will later be used in order to find out which variables, in the sense of this model, have a comparatively high influence on the level of forecast errors.
As with most statistical methods, for OLS certain conditions must be met in order to be able to interpret the results. A violation of one of these conditions usually leads to the fact that the interpretability of our model is reduced (the estimator could for example be biased). For a OLS, the following general assumptions must be met:

- Linear relationship between the variables: As the name suggests, multiple linear regressions, examines the strength of linear relationships.

- No multicollinearity: In the case of multicollinearity, two or more of the predictors correlate strongly with one another. This means that one variable can be predicted from the other with high accuracy. It leads to large variances of the estimated coefficients. This was investigated by looking at the correlation between all combinations of explanatory variables for all models. The only correlation "that seems to be significant enough" is the one between the load forecast FC_{Load} and the day ahead price $price_{DA}$ with a value of 0.618. However, the bad condition number of the matrix $X'X$ (see table 5.2) shows that some columns of X may be explained almost perfectly by a linear combination of the other columns. This again leads to large variances of the estimates.

- No outliers: Outliers are a problem for most parametric statistical methods. A single outlier can destroy an otherwise significant trend. Looking at the data some outliers can be observed - but only a low amount.

Considering linear relationship between the variables, the corresponding errors must fulfill the following properties:

- Uncorrelated errors: Autocorrelation of the errors is a wide- spread problem for many reasons. Autocorrelation reduces the informative value of our results.

- Homoscedasticity (equality of variances) of the errors: OLS estimation expects the variance of the errors to be the same. If this condition is violated, the model explains one section of the data better than another.

- Normal distribution of the errors: The errors should not only be uncorrelated and homoscedastically distributed, but also (roughly) normal distributed.

The multiple linear regression for the forecast errors was implemented in *R* [R Core Team, 2013] using *lm* from the STATS package [Team, 2012].

This enables the possibility to investigate whether the previously mentioned assumptions are fulfilled for the given dataset. Figure 5.1 shows the residuals vs. the fitted values of all three multiple linear regression models. This can be used to check the **linear relationship between the variables**. A horizontal line without any "clustered" deviations from that line (or other visible patterns) indicate a linear relationship. The wind model plot showcases a horizontal line, but with largely increasing spread of residuals for higher fitted values. Both the load as well as the solar plot do not seem to indicate a linear relationship.

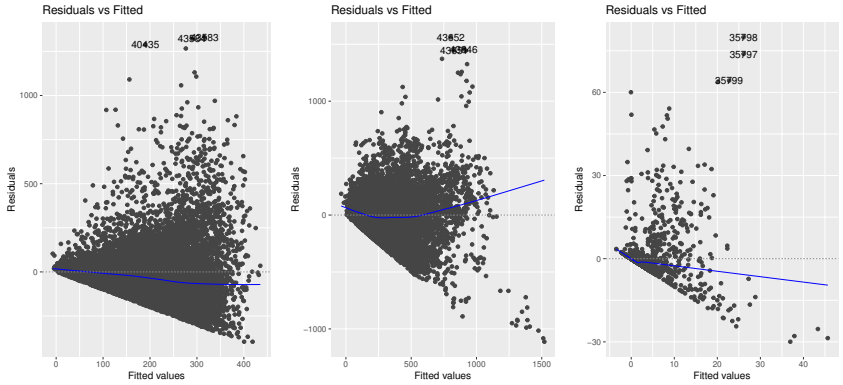

(a) Wind (b) Load (c) Solar

Figure 5.1: Residuals vs. fitted values for the multiple linear regression, showcasing clear patterns for all three variables - indicating that the relationship may not be fully linear.

Figure 5.2 shows the Scale-Location plot (left column) and the Normal QQ-plot (right column) for the wind, load and solar multiple linear regression model. After visualizing the indication of linear relationships in the previous plot, the Scale-Location plots the square root of the absolute standardized residuals[1] against the fitted values. This can be used as indicator for **homoscedasticity** (homogeneity of the variance of the residuals). The non-horizontal line, with increasing spread, in all plots indicates heteroscedasticity for all three models. The Normal QQ-plots can be used to compare the quantiles of the residuals against the theoretical quantiles of a normal distribution. If the quantiles "match" (indicated by all points lying on the 45° line), this can indicate that the "**normal distribution of the residuals**" assumption holds. It can be observed that this assumption is violated, where especially for the solar model huge deviations from the theoretical quantiles can be observed. This is due to the fact, that a high number of zeros are present in the observation (hours were the solar forecast was "perfect"), but at the same time outliers with huge forecast errors exist (see the right plot of figure 5.2b).

[1]The "standardized residuals" in the implementation of *lm* in R refer to the studentized residuals $\frac{\hat{\epsilon_i}}{\hat{\sigma}\sqrt{1-h_{ii}}}$, where $\hat{\sigma}^2 := \frac{1}{n-m}\sum_{j=1}^{n}\hat{\epsilon_i}^2$ and m is the column dimension of X. h_{ii} is the so called leverage and is defined as $h_{ii} := (X(X'X)^{-1}X')_{ii}$. This is a measure of the influence that the observed response y_i has on its predicted value $\hat{y}_i$.

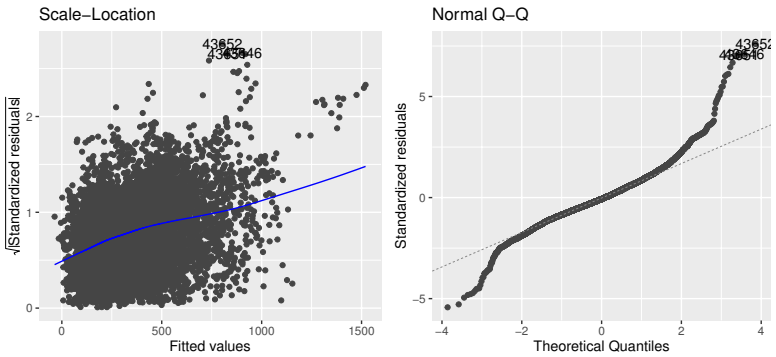

(a) Load

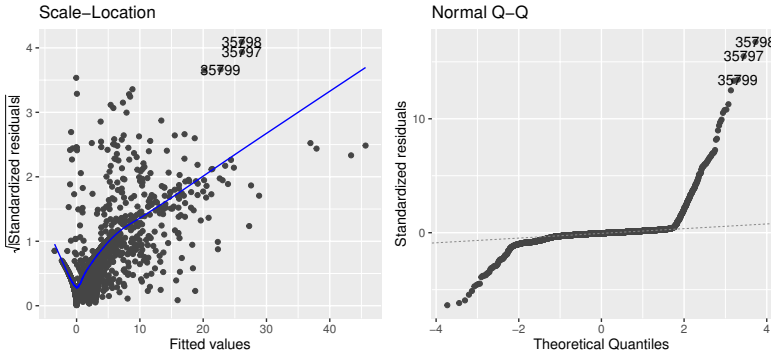

(b) Solar

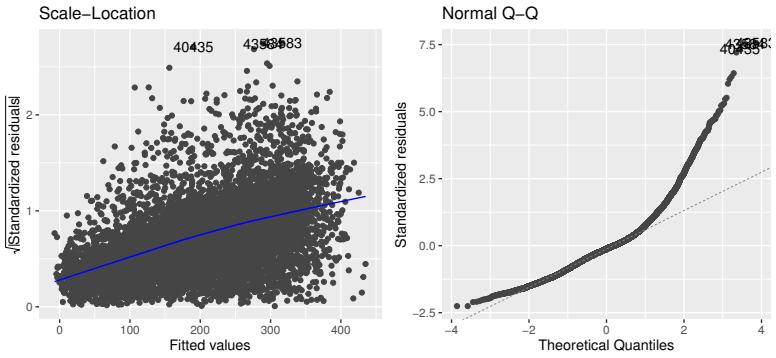

(c) Wind

Figure 5.2: Scale-Locations (that hint to the presence of heteroscedasticity due to a non constant relation being displayed) and Normal QQ-plots (that show that the residuals do not follow a normal distribution for any of the three variables) for the multiple linear regression.

Furthermore the **independence of the residuals** can be investigated using the Durbin-Watson test. The Durbin-Watson test is a statistical test commonly used to test for autocorrelation of residuals with lag 1. The null hypothesis states that there is no correlation among residuals, while the alternative hypothesis is that residuals are autocorrelated. As table 5.3 shows, the null hypothesis is rejected in all three cases, implying the possible existence of autocorrelation of residuals.

Table 5.3: Durbin-Watson test indicating a positive autocorrelation of residuals.

Model	Autocorrelation	p value
Wind	positive	0
Load	positive	0
Solar	positive	0

The default implementation uses the mentioned two sided test (with the alternative hypothesis only stating that there is an autocorrelation). The sign of the autocorrelation can be checked by performing a one sided test (fixing the alternative hypothesis to either an autocorrelation greater or less than zero), which clearly indicates a positive autocorrelation (p value of 0 vs. a p value of 1 when checking for negative autocorrelation). It can further be investigated whether there is autocorrelation for lags greater than 1. This was done for all lags up to 24. This rejects the null hypothesis (indicating autocorrelation of residuals) for all lags up to 6, with some lags greater than 6 not rejecting the null hypothesis.

Tobit Model

The tobit model tries to describe the relationship between variables, where the dependent variable is constrained in a certain sense. The usual restriction mechanisms here are "truncation" and "censoring". A truncated variable is only observable in a particular range (e.g. income tax as a percentage of income in Austria), a censored variable only to a certain extent (e.g. lifetime of machine parts). Latent variables are often used with tobit models in which y^* is directly observable. However a function y of the latent variable y^* can be observed. An example for such a variable is the student knowledge in a specific subject area. It can neither be observed nor is it exact quantifiable, but assessments of exams and written works could be understood as estimates of it.
Let y^* be a latent random variable and let y be observed. y is left-censored for

L, if

$$y = \begin{cases} y^* & y^* > L \\ L & y^* \leq L \end{cases}$$

respectively y is left-truncated for L, if

$$y = y^* \quad y^* > L$$

There are a lot of different tobit models which allow different modeling of connections or the data itself. The first tobit model was developed for the analysis of cross-sectional data from households, but such models have already been used in the context of time series analysis. In this thesis the focus of consideration is the standard tobit model (also called tobit-I model) [Schneider, 2019].

Since all considered absolute forecast errors are by definition non-negative, the used data can be interpreted as being left-censored at $L = 0$. This suggests applying a tobit model as additional way to estimate the coefficients. Since values of $y_i = 0$ only exist for the solar forecast error, the tobit model was not conducted for the load and wind forecast error (where it would lead to the same results as the multiple linear regression).
The standard tobit model for the forecast error was implemented in *R* [R Core Team, 2013] using *tobit* from the AER package [Kleiber and Zeileis, 2020]. L (the lower bound) was defined as zero and a left-censored tobit model is chosen. The coefficients β of the underlying multiple linear regression are estimated using the IRLS (iteratively reweighted least squares) algorithm that implements a maximum likelihood estimation.

Quantile Regression

Quantile regression (QR) [Koenker and Bassett Jr, 1978] is a method for estimating functional relations between variables for all portions of a probability distribution.
This type of modeling represents a good alternative to conventional regression. Restrictive assumptions such as, for example, a certain distribution for the error terms are not necessary anymore. Furthermore, the estimator of the conditional quantile function provides a more thorough overview of the response's distribution (achieved by estimating coefficients for multiple quantiles) than it

is the case with models that only consider the conditional expected value (like OLS). The following summary of the backgrounds of quantile regression is based on [Körbler, 2014].
Quantiles are used to describe the distribution of the dependent variable. Quantiles and percentiles are used synonymously - the 0.99 quantile is the 99^{th} percentile. The best-known quantile is the median, which is the 0.50 quantile.
For a fixed value of $\tau \in (0, 1)$ - the quantile one is interested in estimating - and assuming a so-called *loss function* that is defined as

$$\rho_\tau(y) := y(\tau - \mathbb{1}_{\{y<0\}})$$

the theoretical τ-quantile can be calculated as

$$\arg\min_{q_\tau \in \mathbb{R}} \mathbb{E}(\rho_\tau(Y - q_\tau))$$

Here, the loss function acts as asymmetric, weighted absolute value function. Choosing $\tau = 0.5$ for example leads to a symmetric function (as can be seen by the definition) and to the calculation of the median.
When looking at regression tasks, obviously the true distribution of the outcome variable Y is not known. Therefore the empirical cdf must be used. Assuming that y_i are the observations of Y, this leads to solving the minimization problem (for the derivation see [Körbler, 2014]):

$$\hat{q}_\tau = \arg\min_{q_\tau \in \mathbb{R}} \frac{1}{n} \sum_{i=1}^{n} \rho_\tau(y_i - q_\tau)$$

The calculation of this (empirical) quantile can be reformulated as LP (linear program). This follows the idea that by defining

$$r_i := y_i - q_\tau$$

and replacing this residual term by the difference of two non-negative variables u_i, v_i so that

$$r_i = u_i - v_i$$

it can be followed that

$$\rho_\tau(y_i - q_\tau) = \rho_\tau(r_i) = \tau u_i + (1 - \tau)v_i$$

This can now be formulated as LP:

$$\begin{aligned} \min_{q_\tau,u,v} \quad & \sum_{i=1}^{n} \tau u_i + (1-\tau)v_i \\ \text{s.t.} \quad & q_\tau + u_i - v_i = y_i \quad \forall i \end{aligned}$$

The explained approach can now be formulated in a more general way to account for explanatory variables (captured in the regression matrix X) by considering *conditional* quantiles. This is done by replacing the ("static") quantile function q_τ by its conditional counterpart $Q_Y(\tau|x) = x'\beta_\tau$ for any given vector x of observed explanatory variables. Using the i-th row of the regression matrix X, given by $x_{i\cdot}$, the estimator $\hat{\beta}_\tau \in \mathbb{R}^k$ is again determined through solving a LP minimization:

$$\begin{aligned} \min_{\beta_\tau,u,v} \quad & \sum_{i=1}^{n} \tau u_i + (1-\tau)v_i \\ \text{s.t.} \quad & x_{i\cdot} \cdot \beta_\tau + u_i - v_i = y_i \quad \forall i \end{aligned}$$

For the j^{th} regressor, the marginal effect is the coefficient for the τ-quantile, written as follows

$$\frac{\partial Q_Y(\tau|x)}{\partial x_j} = \beta_{\tau,j}$$

A quantile regression parameter $\beta_{\tau,j}$ estimates the change of a specified quantile τ of the dependent variable y produced by a one unit change in the independent variable x_j. The marginal effects are for infinitesimal changes in the regressor, assuming that the dependent variable remains in the same quantile.
Unlike interpretations of OLS estimation, the interpretation of quantile regression results need to specify which quantile of the dependent variable they refer to. QR coefficients can be significantly different for some or all quantiles in comparison with results form the OLS.

The quantile regression will be used later on, in order to find out which variables, in the sense of this model, have a comparatively high influence on the level of forecast errors. The quantile regression for the forecast errors was implemented in *R* [R Core Team, 2013] using *rq* from the QUANTREG package [Koenker, 2021]. The used algorithmic method to compute the fit is "br". This default method is the modified version of the Barrodale and Roberts algorithm for L1-regression and is described in [Koenker and d'Orey, 1994]. This is quite efficient for problems up to several thousand observations, and may be used

to compute the full quantile regression process [Koenker, 2021], [EconometricsAcademy, 2020].

5.1.3 Results

As conclusion of the results from chapter 4 on descriptive data analysis, the data from 2019 and 2020 is considered for the previously introduced models (multiple linear regression, tobit model and quantile regression as explained theoretical in section 5.1.2). The data of 2019 is being used as so-called training data, i.e. to build the models. The data of 2020 is then used as test data to examine the quality of the models. It is important that the training data and test data are disjoint, so as not to test on data that was used to build the models.

Graphic Differences

First, scatter plots are shown in which the predicted absolute forecast value is compared to the historical value of the respective absolute forecast error. The respective scatter plots for the multiple linear regression for the load and wind forecast error are shown.
Figure 5.3 shows the predicted $|FCE_{Load}|$ versus the historic $|FCE_{Load}|$ in the multiple linear regression as well as the predicted $|FCE_{Wind}|$ versus the historic $|FCE_{Wind}|$. In both cases a weak connection between the predicted absolute forecast error and realized absolute forecast error can be seen.

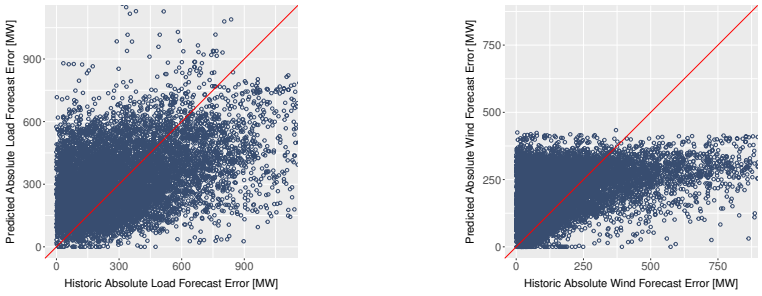

(a) Absolute Load Forecast Error (b) Absolute Wind Forecast Error

Figure 5.3: Scatterplots comparing the predicted vs. realized absolute load and wind forecast error for the multiple linear regression during the test year 2020. While both plots hint at the fact that the model does not capture all variation in the data well, the most prominent observation can be deducted from the wind plot: Absolute forecast errors above 400 MW can not be modelled and are heavily under-predicted.

Figure 5.4 shows the predicted $|FCE_{Solar}|$ versus the historic $|FCE_{Solar}|$ in the multiple linear regression as well as in the tobit model. For the model of $|FCE_{Solar}|$, the results seem rather random.

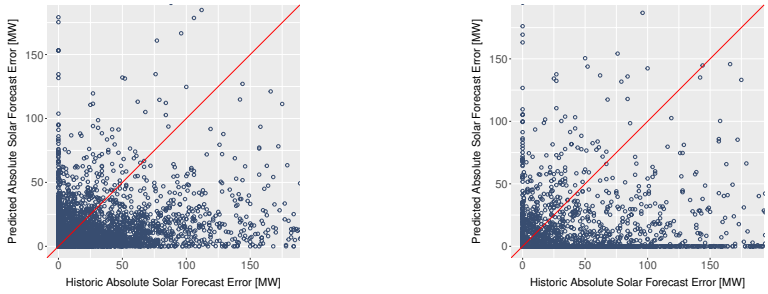

(a) Multiple Linear Regression (b) Tobit Model

Figure 5.4: Scatterplots comparing the predicted vs. realized absolute solar forecast error for the multiple linear regression and the tobit model during the test year 2020. Especially the tobit model displays an excess of predicted zeros.

In figure 5.5 the different results for the most important coefficients concerning the quantile regression for the $|FCE_{Load}|$ are shown and compared with the results for the multiple linear regression.
The red solid line marks the estimator of the coefficient for the respective exogenous variable in the multiple linear regression, while the red dashed line shows the respective standard error. Since in the multiple linear regression the estimator does not differ for the individual quantiles, it is clear that it must be a constant value for the estimator. The blue dashed line shows the respective estimator of the coefficient for the respective quantile in the quantile regression. The gray area indicates the respective standard error. For the quantile regression, all quantiles were calculated with an interval of 5%, starting with the 5% quantile and ending with the 95% quantile.

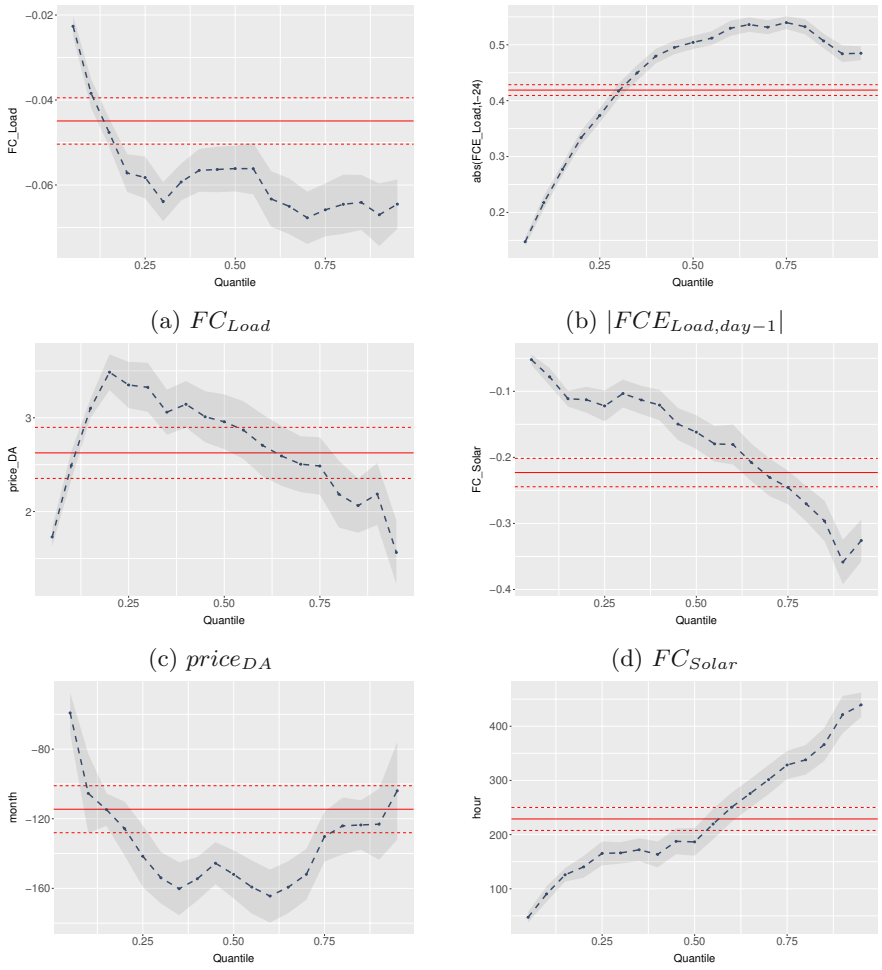

(a) FC_{Load} (b) $|FCE_{Load,day-1}|$

(c) $price_{DA}$ (d) FC_{Solar}

(e) $month - June$ (f) $hour - 12a.m.$

Figure 5.5: Multiple linear regression vs. quantile regression - absolute load forecast error. This highlights the vastly different influence various predictors can have on the outcome variable for different quantiles. It can for example be followed that high day ahead prices have a lower influence on low and high quantiles than they have on the median, suggesting that the distribution above the median actually tightens the higher the day ahead price is.

Graphically it can be clearly seen that the two models perform very differently and the application of quantile regression makes sense. As can be seen in figure 5.5a, approximately around the 15% quantile, the estimator of the coefficient of the quantile regression is significantly below the estimator of the multiple linear regression.

For example, the coefficient for the month (see subfigure 5.5e) is interesting. The month of June was selected as a representative for the presentation. The multiple linear regression returns a higher estimate of the coefficient for approximately 50% of the data. Figure 5.5f also clearly shows the usefulness of the quantile regression. There is a clear difference in the influence of the exogenous variable hour - 12 a.m. in comparison to the results of the multiple linear regression. Clear differences can also be seen for all other subfigures.

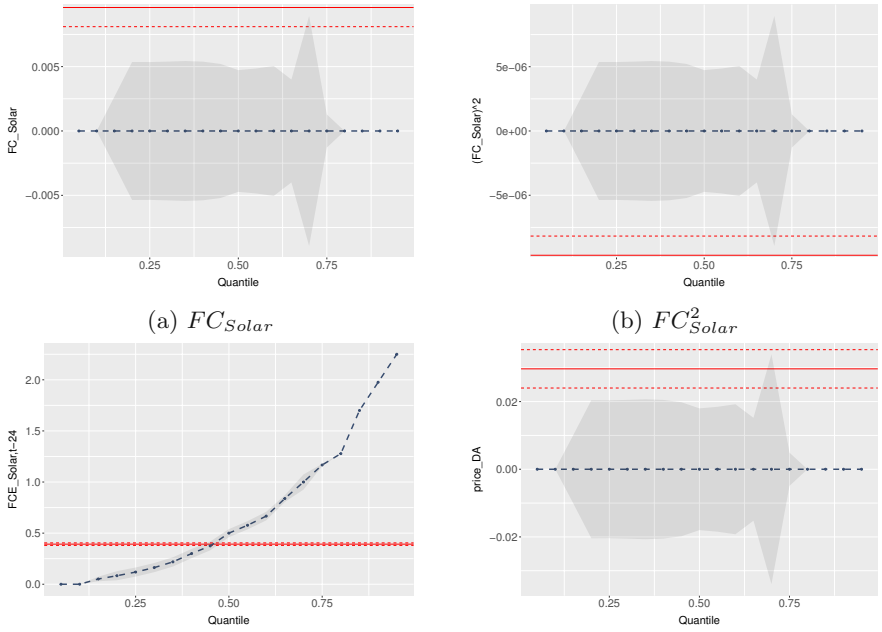

(a) FC_{Solar} (b) FC^2_{Solar}

(c) $|FCE_{Solar,day-1}|$ (d) $price_{DA}$

Figure 5.6: Multiple linear regression vs. quantile regression - absolute solar forecast error. These comparisons show that the quantile regression estimates the effect of the lagged solar forecast error (of the previous day) completely different compared to the multiple linear regression: While the median's estimator is similar, high forecast errors increasingly influence the upper quantiles. This entails that days following "bad forecast days" can result in an estimated distribution that is much wider than for days following "perfect forecast days".

In figure 5.6 the different results for the most important coefficients concerning the quantile regression of the $|FCE_{Solar}|$ are shown and compared with the results for the multiple linear regression. In the case of the coefficients to be estimated for the model of $|FCE_{Solar}|$ it can be seen that for FC_{Solar}, FC^2_{Solar}

and $price_{DA}$ the coefficients for all quantiles are estimated to be zero and also a large standard deviation can be seen. A different picture emerges exclusively for $|FCE_{Solar,day-1}|$. The multiple linear regression returns a higher estimate of the coefficient for approximately 50% of the data and a lower estimate for the rest.

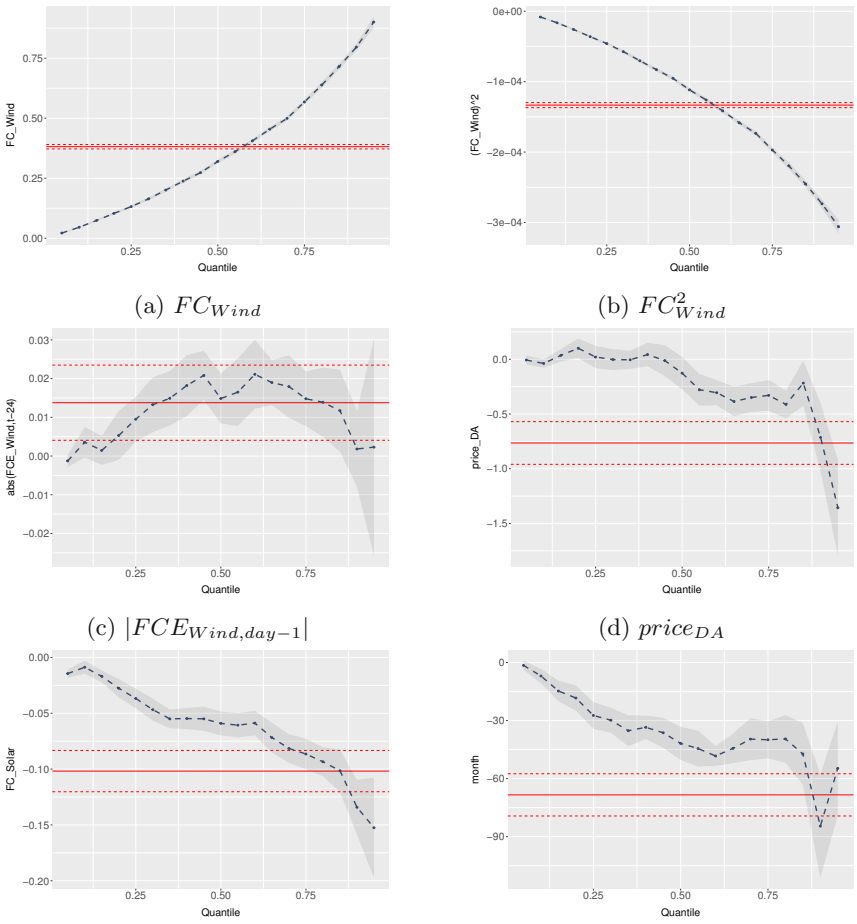

(a) FC_{Wind} (b) FC^2_{Wind}

(c) $|FCE_{Wind,day-1}|$ (d) $price_{DA}$

(e) FC_{Solar} (f) $month - June$

Figure 5.7: Multiple linear regression vs. quantile regression - absolute wind forecast error. Again, significant difference between the estimator can be observed. The coefficients of the wind generation forecast (a) show that high forecasts come with a much wider distribution of absolute wind forecast errors, indicating increased uncertainty during such hours.

In figure 5.7 the different results for the most important coefficients concern-

ing the quantile regression of $|FCE_{Wind}|$ are shown and compared with the results for the multiple linear regression. Also for $|FCE_{Wind}|$ the results show clear differences between the estimators of the multiple linear regression and the quantile regression, which also suggests the use of quantile regression. The conclusion, that in the considered case for the absolute load and wind forecast error quantile regression is useful, can also be supported by the results of the calculation of the MAE and RMSE in section 5.1.3.

Influence of the Variables in the Model

Now an overview of the influence of individual variables on the different regression models is given and the significance of the variables is discussed. As explained in section 5.1.1 three mathematical models (absolute load, solar and wind forecast error) are formulated. For these models three different regression models (multiple linear regression, tobit model, quantile regression) are used to evaluate the influences of the different variables in the model. The tobit model was only used for $|FCE_{Solar}|$. Tables 5.4, 5.5 and 5.6 compare the results of the coefficient estimation of the different used regression models. From now on for the comparison the results of the quantile regression for the 50% quantile (median) are used.
First, $|FCE_{Load}|$ is considered in table 5.4. 8760 observations were considered and embedded in the two different regression models. The two different models for $|FCE_{Load}|$ deliver very similar results. All exogenous variables are marked as significant in both models, which is indicated by a p-value below 0.01. Most of the coefficients of the hours, days and months that are not explicitly listed in the table 5.4 also prove to be significant. The relationships explained by both models are as follows:

- The greater FC_{Load}, the smaller $|FCE_{Load}|$.
- The greater $FCE_{Load,day-1}$, the greater $|FCE_{Load}|$.
- The higher $price_{DA}$, the greater $|FCE_{Load}|$.
- The greater FC_{Solar}, the smaller $|FCE_{Load}|$.

R^2 is the coefficient of determination of the regression. The value of the coefficient of determination indicates the portion of the sum of squares (sum of the squared values of the dependent variables = total sum of squares (TSS)) that is explained by the model. A small coefficient of determination ($R^2 \approx 0$, close to 0) means a poor approximation of the absolute load forecast error by

the linear function of the independent variables. A high coefficient of determination ($R^2 \approx 1$) means that $|FCE_{Load}|$ is well explained by a linear function of the independent variables [Scherrer, 2015]. In the multiple linear regression for $|FCE_{Load}|$, $R^2 = 0.473$. The use of an adjusted R^2_{adj} is an attempt to account for the phenomenon of the R^2 automatically and spuriously increasing when extra explanatory variables are added to the model. Here adjusted R^2_{adj} and R^2 have approximately the same value.

For the multiple linear regression model, many software packages (also in R) automatically output an F-statistic. This is the corresponding statistic to test:

$$H_0 : \beta_1 = ... = \beta_k = 0 \text{ vs. } H_1 : \beta_j \neq 0 \text{ for minimum one } 1 \leq j \leq k,$$

where β_0 is the intercept. This is often referred to as "testing the significance of the regression", because it tests whether a constant alone, without exogenous variables, describes the data just as well. The F-statistic is calculated using the restricted OLS estimator with the restriction determined by H_0 [Schneider, 2019]. Here (multiple linear regression) the F-statistic has the value 177.465 and is significant. For the 50% quantile, the quantile regression provides results that are very similar to the multiple linear regression model.

In table 5.5 $|FCE_{Solar}|$ was considered. 5200 observations were considered and embedded in the various regression models. The number of observations is lower than in the models for the absolute load or wind forecast error, since all values for which FC_{Solar} is equal to zero have been removed[2]. One can say that the quantile regression for $|FCE_{Solar}|$ is performing poorly. The reason is that FCE_{Solar} is zero most of the time, hence the median is zero and so the results for the 50% quantile for the different estimated parameter for the exogenous variables are zero. See figure 5.6, the estimated coefficients are also zero when considering other quantiles (except the coeffient for $|FCE_{Solar,day-1}|$). When comparing the results for the mean absolute error (MAE) and the root mean square error (RMSE) on the out-of-sample test dataset, the quantile regression performs clearly best according to MAE and second best according to the RMSE just behind the multiple linear regression.

[2]During the six years (2015-2020) a total of ten hours were recorded for which the realized solar generation was not exactly zero, even though the forecast was zero. This entails that the best possible forecast that can be made for $|FCE_{Solar}|$ during hours where $FC_{Solar} = 0$ is zero.

Table 5.4: Results: Absolute load forecast error, results of quantile regression given as estimation of the 0.5 quantile. Both models (MLR and QR) estimate the same signs for all coefficients and indicate that all of them are significant. The regressions for $|FCE_{Load}|$ result in the highest R^2 (compared to the other two stage I models).

	Dependent variable:	
	$\|FCE_{Load}\|$	
	Multiple Linear Regression	*Quantile Regression*
	(1)	(2)
FC_{Load}	-0.045^{***}	-0.056^{***}
	(0.005)	(0.005)
$\|FCE_{Load,day-1}\|$	0.419^{***}	0.504^{***}
	(0.010)	(0.012)
$price_{DA}$	2.626^{***}	2.958^{***}
	(0.272)	(0.292)
FC_{Solar}	-0.223^{***}	-0.162^{***}
	(0.021)	(0.026)
Intercept	374.798^{***}	420.667^{***}
	(30.899)	(32.243)
Observations	8,760	8,760
R^2	0.473	
Adjusted R^2	0.470	
Residual Std. Error	206.108 (df = 8715)	
F-Statistic	177.465^{***} (df = 44; 8715)	
Note:		*p<0.1; **p<0.05; ***p<0.01

For $|FCE_{Solar}|$ a tobit model was created. The multiple linear regression model and the tobit model also provide different values for the coefficients:

- In both cases, the influence of the solar forecast is significant with a positive influence and the square of the FC_{Solar} and the $|FCE_{Solar,day-1}|$ are also significant with the same sign.
- There are clear differences in $price_{DA}$. In the multiple linear regression, the coefficient for $price_{DA}$ has a positive influence, while in the tobit model a negative influence can be seen.
- In both cases, the influence of $price_{DA}$ is significant.
- The same phenomenon that the signs of the estimated coefficients are different is shown concerning *hour* and $hour^2$. This shows that $|FCE_{Solar}|$

for the multiple linear regression model is lowest shortly after noon. Conversely, estimating the coefficients using the tobit model shows that $|FCE_{Solar}|$ is greatest shortly before noon and is lower in the evening and morning hours. In the multiple linear regression, $|FCE_{Solar}|$ is lowest in the morning, while in the tobit model the minimum is reached a little later.

- The coefficients in the multiple linear regression model or in the tobit model are negative for $month$ and positive for $month^2$.

The coefficient of determination R^2 can also be calculated in this multiple linear regression. R^2 has the value 0.316, while the adjusted coefficient of determination R^2_{adj} has the value 0.315. The value of the F-statistic is shown as significant. In the tobit model, the value of the Wald-Test can be viewed as significant as well.
Finally, the results of the models for $|FCE_{Wind}|$ are considered. 8760 observations were considered and embedded in two different regression models (multiple linear regression, quantile regression). It can be seen that the models for $|FCE_{Wind}|$ deliver very similar results. Most of the coefficients of the exogenous variables are marked as significant in both models, which means that the p-value is below 0.01. Most of the coefficients of the hours, days and months that are not explicitly listed in the table 5.6 also prove to be significant. The relationships explained by both models (see figure 5.4) are as follows:

- The greater FC_{Wind}, the greater $|FCE_{Wind}|$. The greater FC^2_{Wind}, the smaller $|FCE_{Wind}|$. That means, higher FC_{Wind} increases the expected FC_{Wind} up to a forecast of around 2000 MW. From here on, there is a decreasing influence on the $|FCE_{Wind}|$.
- The greater $|FCE_{Wind,day-1}|$, the greater $|FCE_{Wind}|$.
- The higher $price_{DA}$, the lower $|FCE_{Wind}|$.
- The greater FC_{Solar} (this is mostly an indicator for "good", stable and warm weather), the smaller $|FCE_{Wind}|$.

The coefficient of determination R^2 can also be calculated in this multiple linear regression. R^2 has the value 0.218, while the adjusted coefficient of determination R^2_{adj} has the value 0.215. The value of the F-statistic is shown as significant. For the 50% quantile, the quantile regression provides results that are very similar to the multiple linear regression.

Table 5.5: Results: Absolute solar forecast error, results of quantile regression given as estimation of the 0.5 quantile. While the QR only estimates one coefficient distinct from zero, both MLR and the tobit model indicate most coefficients to be significant. Large differences in estimations (partially with varying signs) between these two models can be observed. Only 5200 out of 8760 observations were used due to omitting hours for which $FC_{Solar} = 0$.

	Dependent variable:		
	$\lvert FCE_{Solar}\rvert$		
	Multiple Linear Regression	*Tobit Model*	*Quantile Regression*
	(1)	(2)	(3)
FC_{Solar}	0.010^{***}	0.026^{***}	0.000
	(0.001)	(0.007)	(0.013)
FC^2_{Solar}	-0.00001^{***}	-0.0001^{***}	−0.000
	(0.00000)	(0.00001)	(0.00002)
$\lvert FCE_{Solar,day-1}\rvert$	0.392^{***}	0.530^{***}	0.500^{***}
	(0.012)	(0.034)	(0.105)
$price_{DA}$	0.030^{***}	-0.066^{***}	0.000
	(0.006)	(0.023)	(0.015)
$hour$	-0.370^{*}	3.661^{***}	0.000
	(0.211)	(0.973)	(1.273)
$hour^2$	0.014^{*}	-0.151^{***}	−0.000
	(0.008)	(0.039)	(0.053)
$month$	-1.842^{***}	-7.236^{***}	−0.000
	(0.157)	(0.659)	(0.925)
$month^2$	0.120^{***}	0.365^{***}	0.000
	(0.012)	(0.051)	(0.097)
$Intercept$	6.001^{***}	−7.048	0.000
	(1.349)	(5.990)	(7.284)
Observations	5,200	5,200	5,200
R^2	0.316		
Adjusted R^2	0.315		
Log Likelihood		-4,400.691	
Residual Std. Error	4.807 (df = 5191)		
F-Statistic	299.861^{***} (df = 8; 5191)		
Wald-Test		$1{,}312.210^{***}$ (df = 8)	
Note:			*p<0.1; **p<0.05; ***p<0.01

Table 5.6: Results: Absolute wind forecast error, results of quantile regression given as estimation of the 0.5 quantile. Both models (MLR and QR) estimate the same signs for all coefficients and indicate that most of them are significant. Out of the three models (load, solar, wind) this one results in the lowest R^2.

	Dependent variable:	
	$\lvert FCE_{Wind}\rvert$	
	Multiple Linear Regression	*Quantile Regression*
	(1)	(2)
FC_{Wind}	0.381^{***}	0.320^{***}
	(0.009)	(0.008)
FC^2_{Wind}	-0.0001^{***}	-0.0001^{***}
	(0.00000)	(0.00000)
$\lvert FCE_{Wind,day-1}\rvert$	0.014	0.015^{**}
	(0.010)	(0.006)
$price_{DA}$	-0.765^{***}	-0.127
	(0.195)	(0.149)
FC_{Solar}	-0.102^{***}	-0.059^{***}
	(0.018)	(0.011)
Intercept	107.647^{***}	67.470^{***}
	(15.737)	(12.856)
Observations	8,760	8,760
R^2	0.218	
Adjusted R^2	0.215	
Residual Std. Error	176.188 (df = 8720)	
F-Statistic	62.452^{***} (df = 39; 8720)	
Note:		*p<0.1; **p<0.05; ***p<0.01

Qualitative Differences

In order to better assess the previously presented results of the models, the following section attempts to highlight qualitative differences. The mean absolute error (MAE) and the root mean squared error (RMSE) are used for this and are defined as:

$$MAE = \frac{1}{n}\sum_{i=1}^{n} |\hat{FCE}_{i,predicted} - FCE_i| \text{ and}$$

$$RMSE = \sqrt{\frac{\sum_{i=1}^{n}(\hat{FCE}_{i,predicted} - FCE_i)^2}{n}},$$

where n is the number of the predicted values, $\hat{FCE}_{i,predicted}$ are the predicted forecast errors and FCE_i are the realized (actual/correct) forecast errors.

The larger either one of them is, the worse the fit of the model. It is therefore important to control influencing factors to obtain the smallest possible MAE/RMSE in order to improve the quality of a model.
The MAE and RMSE are calculated on the test data (whole year of 2020). The results of the calculation of the MAE and RMSE for the different forecast types (Naive Zero, Naive Mean, Lag1, multiple linear regression (MLR), tobit model (Tobit), quantile regression (QR)) for the absolute load, solar and wind forecast error are shown in table 5.7. Naive Zero, Naive Mean and Lag1 are so-called naive forecasts. The Naive Zero model always uses the value zero as forecast, while the Lag1 model always selects the value of the previous day at the same hour as the forecast. The Naive Mean uses the mean of the whole training data (2019) as forecast. The results for these three naive models are now compared with those of the multiple linear regression, the tobit model and the quantile regression.
Since we know that the model fits the data better the lower the value of MAE and RMSE, it can be seen in table 5.7 that the multiple linear regression, the tobit model and the quantile regression provide better results for load, solar and wind forecast errors than the naive forecasts. In the case of absolute load and wind forecast error, the quality of the forecast is significantly improved by the quantile regression.
For $|FCE_{Solar}|$, only a slight improvement in quality compared to the Naive Zero model can be recognized, which is due to the fact that the solar forecast error is zero most of the time and therefore the results apply quite well with the naive forecast. In table 5.7 also the results for the quantile regression (for the 50% quantile) are shown. Overall the quantile regression seems to be performing quite good, with being the best for $|FCE_{Load}|$ and also really good for $|FCE_{Solar}|$ and $|FCE_{Wind}|$.

Table 5.7: Comparison - MAE and RMSE. **Bold** values indicate the best performing "model" for each column. Both MAE and RMSE are better the smaller they are. Mean absolute errors of the forecast errors are identical to the results of the MAE using Naive Zero.

Model	$\lvert FCE_{Load}\rvert$		$\lvert FCE_{Solar}\rvert$		$\lvert FCE_{Wind}\rvert$	
	MAE	RMSE	MAE	RMSE	MAE	RMSE
Naive Zero	338.28	439.93	24.37	55.36	204.78	303.07
Naive Mean	203.35	305.03	24.35	55.34	221.01	314.27
Lag1	187.44	289.29	26.72	60.61	200.05	303.26
MLR	183.12	259.39	22.43	**50.69**	130.97	**204.28**
Tobit	-	-	24.19	53.62	-	-
QR	**177.71**	**256.20**	**22.27**	51.02	**126.82**	208.64

5.1.4 Conclusion

In this chapter, the absolute load, solar and wind forecast error were examined with the help of three different regression models (multiple linear regression, tobit model, quantile regression). It has been shown that carrying out these models as preparation for stage II (investigation of the control area imbalance) makes perfect sense, since all three models deliver significantly better results than the three naive forecasts, Naive Zero, Naive Mean and Lag1.

5.2 Stage II - Control Area Imbalance

In stage II of the model the influences of explanatory variables on the necessary amount of energy in the control area is examined. Two mathematical methods (multiple linear regression and quantile regression) are considered in order to analyze the absolute control area imbalance. The aim of this section is to analyze the balancing energy demand (except FCR) with a focus on renewable energies (solar and wind). The results from stage I for the load, solar and wind forecast errors are used in order to be able to describe their influence on the absolute control area imbalance.

As already mentioned in 4.2 the data on the control area imbalance was taken from the APG website [APG, 2020]. From now on the data for the control area imbalance from 2019 and 2020 is used. The following section gives a complete overview about the mathematical models that are used, including all explanatory variables. Later on some insights into different ways of estimating the unknown coefficients are presented and the chapter concludes with an in-depth analysis of model results and compares the outcomes using the MAE and RMSE.

5.2.1 Mathematical Model

It can be observed that expected value of the control area imbalance is zero, due to the fact that "demand = generation" must be respected at all times. This is one major regulatory requirement that is continuously verified by the E-Control. Otherwise the control area would be unbalanced from the beginning, which could be accounted for without the need for balancing energy. This entails that predicting the direction of the control area imbalance (if there is a surplus or deficit during that specific hour) could potentially be impossible. Therefore the absolute deviation from zero of the control area imbalance is considered. Since this corresponds to a surplus or deficit of energy during a specific timeframe it is still a matter of high importance - even if the direction is not defined - since the magnitude plays a large role for various fields (e.g. power grid security and stability could be at risk if the predicted amount exceed the already procured balancing capacity).

In order to be able to examine the absolute control area imbalance using a multiple linear regression and a quantile regression, first of all the mathematical model that is used in stage II is defined. This model is intended to describe the endogenous variable (absolute control area imbalance) by exogenous variables that are listed below. The chosen explanatory variables were selected based on the results from chapter 4 and from section 5.1.

The thesis is based on the assumption that the absoluteload, solar and wind forecast errors have an influence on the absolute control area imbalance. That is also the reason for the detailed consideration in stage I. Thus these absolute forecast errors are also used as explanatory variables for the construction of the mathematical model. Both the absolute forecast errors of the corresponding day and those of the previous day are used as explanatory variables. That the absolute forecast error of the previous day could have a significant influence is concluded from the autocorrelation in figure 4.2 of the control area imbalance. The realized forecast errors values are used to build the model on the training data. Since these realized values are obviously not available during prediction (that happens during the evening of the day ahead of delivery), these values are replaced by the "best estimate". This best estimate is the result calculated by the models developed in stage I.

Besides the forecast errors, the absolute load, solar and wind forecasts are included to control for any direct effects of these variables. Similar, the day ahead price is include as exogenous variable. It is not immediately obvious at this point, whether this market price exhibits any explanatory power. As a precaution it is therefore taken into account and its significance is evaluated later on,

based on the results of the regression models (table 5.9 and 5.10 show that the inclusion of the day ahead price makes sense).
Finally, the descriptive analysis of the control area imbalance suggests that the considered hour and the respective weekday and month also have a different influence on the absolute control area imbalance. Therefore, these variables are included. To capture individual temporal effects (instead of only describing a direct linear relationship), these are included as dummy variables (similar to stage I) in the mathematical model. Table 5.8 lists the used abbreviations.

Table 5.8: Abbreviations - Stage II

Abbreviation	**Description**
FC_i	Forecast of various variables: $i \in \{Load, Solar, Wind\}$
FCE_i	Forecast Error of various variables: $i \in \{Load, Solar, Wind\}$
$FCE_{i,day-1}$	Lagged Forecast Error of various variables $i \in \{Load, Solar, Wind\}$. This uses the forecast error that occured on the previous day during the same hour (therefore "$day-1$").
$FCE_{i,day-7}$	Lagged Forecast Error of various variables $i \in \{Load, Solar, Wind\}$. This uses the forecast error that occured on the same day of the last week during the same hour (therefore "$day-7$").
$price_{DA}$	Day ahead price published on EPEX Spot
CAI	Control area imbalance; it equals the algebraic sum of all balancing group deviations (aFRR, mFRR, unintentional exchange).
$hour$	Hour of the day
$hour_h$	$hour_h = 1$ if $hour = h$, 0 otherwise
$month$	Month of the year
$month_h$	$month_h = 1$ if $month = h$, 0 otherwise
$wday_d$	$wday_d = 1$ if the day of the week is d, 0 otherwise
u	Residuals

The chosen model for the absolute control area imbalance is as follows (later also called "full" model in this thesis, to describe the fact that all available variables are used):

$$\begin{aligned}|CAI| = \; & \beta_0 + \beta_1 \cdot FC_{Wind} + \beta_2 \cdot FC_{Solar} \\ & + \beta_3 \cdot FC_{Load} + \beta_4 \cdot price_{DA} \\ & + \sum_{h=1}^{24} \beta_{5,h} \cdot hour_h + \sum_{m=1}^{12} \beta_{6,m} \cdot month_m \\ & + \sum_{d=1}^{7} \beta_{7,d} \cdot wday_d \\ & + \beta_8 \cdot |CAI_{day-1}| + \beta_9 \cdot |CAI_{day-7}| \\ & + \beta_{10} \cdot |FCE_{Load}| + \beta_{11} \cdot |FCE_{Load,day-1}| \\ & + \beta_{12} \cdot |FCE_{Solar}| + \beta_{13} \cdot |FCE_{Solar,day-1}| \\ & + \beta_{14} \cdot |FCE_{Wind}| + \beta_{15} \cdot |FCE_{Wind,day-1}| + u\end{aligned} \tag{5.4}$$

In the first step, a multiple linear regression and a quantile regression are applied to the "full" model defined above. Some estimated coefficients of the explanatory variables are clearly not significant in the respective mathematical methods (multiple linear regression, quantile regression: coefficients are estimated for the 50% quantile) that are used (see also results in table 5.9 and 5.10, explained in more detail later in this thesis). Variables that have insignificant coefficients[3] are deleted for the respective method used. This results in two new "short" mathematical models (5.5) and (5.6) which are explained below. When considering the Akaike-Information-Criterion[4] (AIC) for the "full" models (multiple linear regression and quantile regression) as well as the two "short" models (one for the multiple linear regression (5.5) and the other one for the quantile regression (5.6)), it can be seen that the AIC for the "full" model (5.4) is larger than for the "short" models (5.5) and (5.6). This fact underlines the usefulness of the additional consideration of the "short" models (5.5) and (5.6), since a lower AIC indicates possibly better performance.

[3] Where "insignificant" is determined by a p-value greater than 0.05. For the quantile regression this only looks at the p-values of the considered 50% quantile.

[4] The AIC is used to compare different model candidates. The smaller the AIC, the better the chosen model. A detailed description of the AIC can also be found in [Sakamoto et al., 1986].

The resulting "short" mathematical model for the multiple linear regression is as follows:

$$\begin{aligned} |CAI| = \; & \beta_0 + \beta_1 \cdot FC_{Wind} + \beta_2 \cdot price_{DA} \\ & + \sum_{h=1}^{24} \beta_{3,h} \cdot hour_h + \sum_{m=1}^{12} \beta_{4,m} \cdot month_m \\ & + \sum_{d=1}^{7} \beta_{5,d} \cdot wday_d \\ & + \beta_6 \cdot |CAI_{day-1}| \\ & + \beta_7 \cdot |FCE_{Wind}| + \beta_8 \cdot |FCE_{Wind,day-1}| + u \end{aligned} \tag{5.5}$$

The resulting "short" mathematical model for the quantile regression (of the 50% quantile) is as follows:

$$\begin{aligned} |CAI| = \; & \beta_0 + \beta_1 \cdot FC_{Wind} + \beta_2 \cdot price_{DA} \\ & + \sum_{h=1}^{24} \beta_{3,h} \cdot hour_h + \sum_{m=1}^{12} \beta_{4,m} \cdot month_m \\ & + \sum_{d=1}^{7} \beta_{5,d} \cdot wday_d \\ & + \beta_6 \cdot |FCE_{Solar}| + \beta_7 \cdot |FCE_{Wind}| + u \end{aligned} \tag{5.6}$$

5.2.2 Estimating Coefficients

Two mathematical methods are used to estimate the coefficients of the defined mathematical models for the absolute control area imbalance. On the one hand multiple linear regression and on the other hand quantile regression are used. The more precise theoretical explanation of the two regression models is already given in section 5.1.2. The implementation of the multiple linear regression and the quantile regression is done in *R* [R Core Team, 2013].

5.2.3 Results

As conclusion of the results from section 4.5 on descriptive data analysis, the data from 2019 and 2020 is considered for the previously introduced models (multiple linear regression and quantile regression as explained theoretical in section 5.1.2). The data of 2019 is being used as so-called training data, i.e. to build the models. The data of 2020 is then used as test data to evaluate the

quality of the models. It is important that the training data and test data are disjoint, so as not to test on data that was used to build the models.[5]
Furthermore, the results from stage I for the absolute load, solar and wind forecast errors were used to generate two additional test datasets. In the original test dataset (data from 2020), the real absolute load, solar and wind forecast errors were replaced by the results (predicted forecast errors) of the multiple linear regression (stage I) and in the second dataset by the results (predicted forecast errors) of the quantile regression (just the estimated coefficients for the 50% quantile are used, stage I). This resulted in two more test datasets in addition to the original one featuring the realized (historic) forecast errors.
The aim is to create a forecast for the absolute control area imbalance and the absolute load, solar and wind forecast errors are used as explanatory variables. Since these values are not known at the time of the forecast, therefore it is necessary to predict these forecast errors (see explanations in stage I) and to generate these two additional test datasets.
In order to evaluate the quality of the forecast of the absolute control area imbalance (using the predicted forecast errors), the MAE and RMSE are calculated on the test data 2020 using the real forecast errors as benchmark.
Similar to stage I a Durbin-Watson-Test was applied to check for autocorrelation of the residuals. For all four models (multiple linear regression and quantile regression for the 50% quantile; both times for the "full" as well as the "short" model) the test clearly (p-value $< 3 \cdot 10^{-16}$) rejects the null-hypothesis, indicating that the alternative hypothesis (stating that the autocorrelation is greater than zero) is most likely true.

Graphic Differences

In figure 5.8 two scatter plots for the multiple linear regression and the quantile regression (using the 50% quantile) for the predicted and historic $|CAI|$ for the "full" mathematical model (5.4) are shown. In figure 5.8 for the multiple linear regression the test data using the results of the multiple linear regression in stage I is considered. For the quantile regression the test data using the results of the quantile regression (50% quantile) in stage I is considered.

[5] This results in all timestamps starting at 2019-01-01 00:00:00 until 2019-12-31 23:00:00 belonging to the training set - the set of data that all models are built on - and all timestamps starting at 2020-01-01 00:00:00 until 2020-12-31 23:00:00 making up the test set - the set that the model performance is being evaluated on.

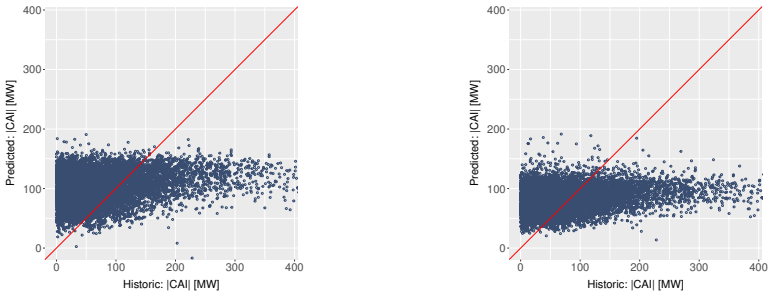

(a) Multiple Linear Regression (b) Quantile Regression

Figure 5.8: Predicted versus realized absolute control area imbalance ("full" models). Both models fail to predict deviations greater than 200 MW.

In figure 5.9 two scatter plots for the multiple linear regression and the quantile regression (using the 50% quantile) for the predicted and historic $|CAI|$ of the "short" mathematical models (5.5) and (5.6) are shown. For the multiple linear regression the test data using the results of the multiple linear regression in stage I is considered. For the quantile regression the test data using the results of the quantile regression (50% quantile) in stage I is considered.

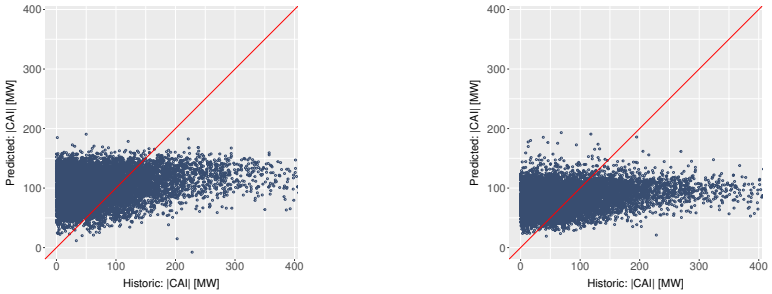

(a) Multiple Linear Regression (b) Quantile Regression

Figure 5.9: Predicted versus realized absolute control area imbalance ("short" models). Both models fail to predict deviations greater than 200 MW.

The other combinations of scatterplots like for example using the test data with the results of the multiple linear regression in stage I for the quantile regression and the other way around are not shown here, because those figures do not differ significantly.
Figure 5.10 compares the estimated coefficients of the multiple linear regression and quantile regression model and is only generated for the "full" mathematical model (5.4), because the "full" model is the same for the multiple linear

regression and the quantile regression, so it is possible to compare the estimated coefficients for some explanatory variables. In case of the two different "short" models (5.5) and (5.6) for the multiple linear regression and the quantile regression a comparison like this is not useful.
The red solid line marks the estimator of the coefficient for the respective exogenous variable in the multiple linear regression, while the red dashed line shows the respective standard error. Since in the multiple linear regression the estimator does not differ for the individual quantiles, it is clear that it must be a constant value for the estimator. The blue dashed line shows the respective estimator of the coefficient for the respective quantile in the quantile regression. The gray area indicates the respective standard error. For the quantile regression, all quantiles were calculated with an interval of 5%, starting with the 5% quantile and ending with the 95% quantile.

Influence of the Variables in the Model

The most important results for the multiple linear regression for the "full" model (5.4) and "short" mathematical model (5.5) are shown in table 5.9. It turns out that the load and solar forecasts are not significant. The $|FCE_{Solar}|$ of the respective day or the previous day is also not significant and is therefore removed in the short model. However, FC_{Wind} and $|FCE_{Wind}|$ for the current day are significant. $price_{DA}$ and $|FCE_{Load,day-1}|$ are also significant. The results for the "full" mathematical model (5.4) led to the "short" mathematical model (5.5) by "clearing" the "full" model (deleting the explanatory variables, which do not have significant coefficients). In table 5.9 it can be seen that the results between the "full" model (5.4) and the "short" model (5.5) do not differ much concerning the signs and magnitudes of the estimated coefficients and that the coefficient of determination is the same for both models.
The most important results for the quantile regression (50% quantile) for the "full" model (5.4) and "short" mathematical model (5.6) are shown in table 5.10.

Table 5.9: Results: Multiple linear regression ("full" vs. "short"). Coefficients missing are due to insignificant variables being omitted from the short model.

	Dependent variable:	
	$\|CAI\|$	
	(full)	(short)
FC_{Wind}	0.007^{***}	0.007^{***}
	(0.001)	(0.001)
FC_{Solar}	0.005	
	(0.009)	
FC_{Load}	0.003	
	(0.002)	
$price_{DA}$	-0.639^{***}	-0.566^{***}
	(0.111)	(0.094)
$\|CAI_{day-1}\|$	0.025^{**}	0.021^{**}
	(0.011)	(0.010)
$\|CAI_{t-7}\|$	0.013	
	(0.010)	
$\|FCE_{Wind}\|$	0.155^{***}	0.154^{***}
	(0.005)	(0.005)
$\|FCE_{Wind,day-1}\|$	-0.005	
	(0.005)	
$\|FCE_{Solar}\|$	0.193	
	(0.234)	
$\|FCE_{Solar,day-1}\|$	-0.021	
	(0.230)	
$\|FCE_{Load}\|$	0.004	
	(0.004)	
$\|FCE_{Load,day-1}\|$	-0.012^{***}	-0.011^{***}
	(0.004)	(0.004)
Constant	76.202^{***}	93.606^{***}
	(12.596)	(7.464)
Observations	8,760	8,760
R^2	0.161	0.161
Adjusted R^2	0.156	0.156
Residual Std. Error	81.248 (df = 8707)	81.246 (df = 8714)
F Statistic	32.197^{***} (df = 52; 8707)	37.063^{***} (df = 45; 8714)
Note:		*p<0.1; **p<0.05; ***p<0.01

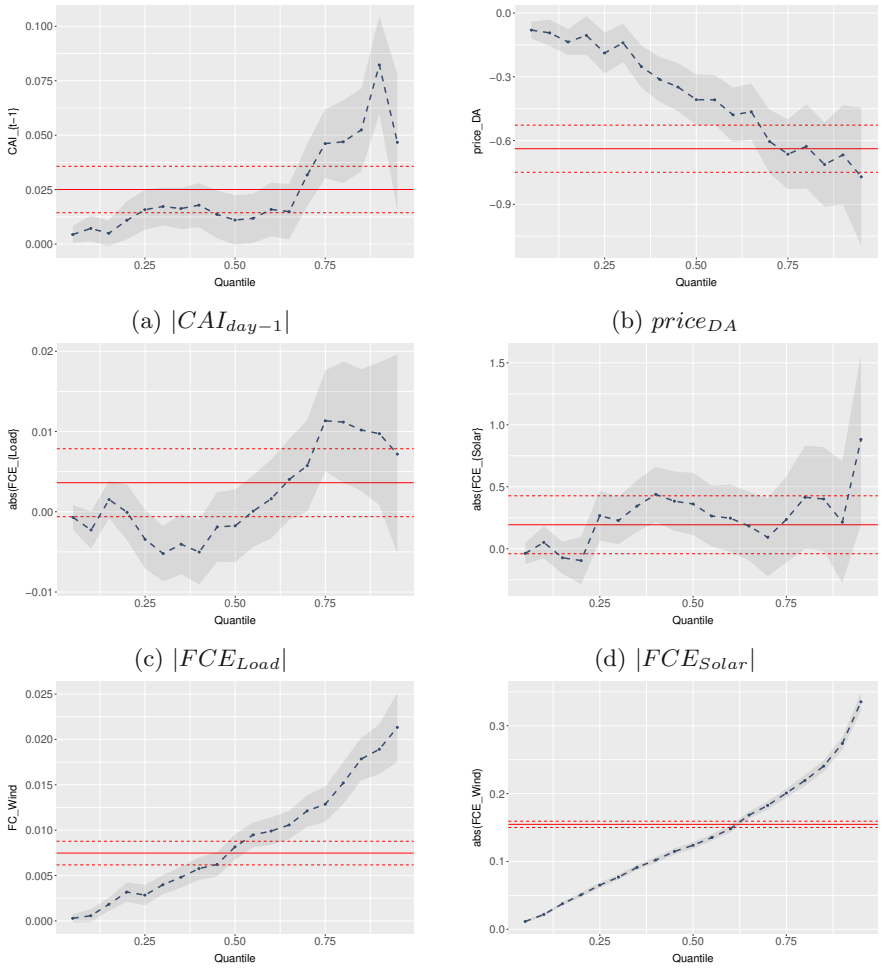

(a) $|CAI_{day-1}|$ (b) $price_{DA}$

(c) $|FCE_{Load}|$ (d) $|FCE_{Solar}|$

(e) FC_{Wind} (f) $|FCE_{Wind}|$

Figure 5.10: Multiple linear regression vs. quantile regression - control area imbalance ("full" model). While $|FCE_{Solar}|$ shows an overlap of the two estimators (indicating that it is not clear whether they differ significantly between the two models), clear differences can be observed e.g. for $|FCE_{Wind}|$. These entail a widening of the estimated distribution ("increased uncertainty") linked to higher absolute wind forecast errors.

Table 5.10: Results: Quantile regression ("full" vs. "short"). Coefficients missing are due to insignificant (for the estimation of the 50% quantile) variables being omitted from the short model. Estimators are more similar compared to the outcome of shortening the MLR. Coefficients for both listed models are estimated for the 50% quantile.

	Dependent variable:	
	$\lvert CAI \rvert$	
	(full)	(short)
FC_{Wind}	0.008^{***}	0.008^{***}
	(0.001)	(0.001)
FC_{Solar}	0.003	
	(0.009)	
FC_{Load}	0.002	
	(0.002)	
$price_{DA}$	-0.408^{***}	-0.371^{***}
	(0.112)	(0.090)
$\lvert CAI_{day-1} \rvert$	0.011	
	(0.010)	
$\lvert CAI_{t-7} \rvert$	-0.0001	
	(0.011)	
$\lvert FCE_{Wind} \rvert$	0.124^{***}	0.124^{***}
	(0.006)	(0.006)
$\lvert FCE_{Wind,day-1} \rvert$	-0.003	
	(0.005)	
$\lvert FCE_{Solar} \rvert$	0.362^{***}	0.335^{***}
	(0.118)	(0.107)
$\lvert FCE_{Solar,day-1} \rvert$	-0.008	
	(0.164)	
$\lvert FCE_{Load} \rvert$	-0.002	
	(0.004)	
$\lvert FCE_{Load,day-1} \rvert$	-0.004	
	(0.004)	
Constant	67.459^{***}	71.717^{***}
	(11.747)	(6.878)
Observations	8,760	8,760
Note:	*p<0.1; **p<0.05; ***p<0.01	

It turns out that FC_{Load} is not significant. The $|FCE_{Solar}|$ of the respective day (in comparison to the multiple linear regression) and FC_{Wind} are significant. $price_{DA}$ is also significant. The results for the "full" mathematical model (5.4) led to the "short" mathematical model (5.6) by "clearing" the "full" model (deleting the explanatory variables, which do not have significant coefficients for the 50% quantile). In table 5.10 it can be seen that the results between the "full" and the "short" model do not differ much.

Quantitative Differences

In order to be able to better assess the previously presented results of the models, the following highlights qualitative differences. The mean absolute error (MAE) and the root mean squared error (RMSE) like in stage I are calculated.
Table 5.11 shows the results of the multiple linear regression for the "full" model (5.4) and the "short" mathematical model (5.5) using the three different test datasets. Of course, the MAE and the RMSE are the smallest for the model on the test data using the historic forecast errors. Since it is the aim to forecast the absolute control area imbalance without knowing the real value of the forecast errors, stage I is needed. The MAE and RMSE on the historic test data are only given as benchmark. In table 5.11 it can be seen that the multiple linear regression performs the best on the test data using the results of the quantile regression (50% quantile) and using the "short" mathematical model (5.5) for the linear regression.

Table 5.11: Multiple linear regression - MAE and RMSE. **Bold** values indicate the best performing model for each row. Both MAE and RMSE are better the smaller they are. Results using historic forecast errors are given as "best-achievable" benchmark.

MLR	**Test-Data (using historic FCE)**		**Test-Data (using results MLR stage I)**		**Test-Data (using results QR stage I)**	
	Full	Short	Full	Short	Full	Short
MAE	59.74	58.77	60.42	60.36	58.70	**58.59**
RMSE	78.20	77.12	80.22	80.18	79.31	**79.21**

Table 5.12 shows the results of the quantile regression for the "full" model (5.4) and the "short" mathematical model (5.6) using the three different test data. It could be expected that the MAE and the RMSE are the smallest for the model on the test data using the historic forecast errors. But the MAE is slightly smaller on the test data using the results of the quantile regression

(50% quantile) for the "full" mathematical model (5.4) as well as for the "short" model (5.6). The RMSE is the smallest for the "full" mathematical model (5.4) on the test data using the results for the multiple linear regression from stage I. When comparing the results from the two tables 5.11 and 5.12, it can be clearly seen that both the MAE and the RMSE have significantly lower values for the quantile regression in stage II and the MAE works best for the "short" model (5.6) on the test data using the results of the quantile regression (50% quantile) from stage I.

Table 5.12: Quantile regression - MAE and RMSE. **Bold** values indicate the best performing model for each row. Both MAE and RMSE are better the smaller they are. Results using historic forecast errors are given as "best-achievable" benchmark.

QR	**Test-Data (using historic FCE)**		**Test-Data (using results MLR stage I)**		**Test-Data (using results QR stage I)**	
	Full	Short	Full	Short	Full	Short
MAE	56.02	56.00	56.10	56.20	**55.43**	55.51
RMSE	76.81	76.70	**78.78**	78.85	78.99	79.04

In table 5.13 the results for the naive forecasts are shown. It shows clearly that the results for the defined models are better than the naive forecasts.

Table 5.13: Naive Forecasts - MAE and RMSE

	Naive Forecasts		
	Naive Zero	Naive Mean	Lag1
MAE	85.60	62.45	77.88
RMSE	118.03	82.32	111.75

5.2.4 Conclusion

In this chapter, the absolute control area imbalance was examined with the help of two different regression models (multiple linear regression and quantile regression) using the results of the absolute load, solar and wind forecast error from stage I. It has been shown that carrying out these models for the absolute control area imbalance makes perfect sense, since all three models deliver significantly better results than the three naive forecasts (Naive Zero, Naive Mean and Lag1). Unfortunately, the "short" model does not perform significantly better than the "full" model when measured using the results for the MAE and RMSE.

It can therefore not be said that removing variables from the initial model improved the models predictive power (but resulted in a smaller model producing similar results for MAE and RMSE). When applying the quantile regression to the test data using the results of the quantile regression (50% quantile) on the defined "full" mathematical model (5.6), overall the best value for the MAE is obtained and when applying the quantile regression to the test data using the results of the multiple linear regression on the defined "full" mathematical model (5.4), overall the best value for the RMSE is obtained.

Chapter 6

Conclusion and Outlook

During the last few years there have been a lot of developments in the electricity market, which affect the requirements on balancing energy. Rising CO_2 emissions and global warming led to an expansion of renewable and sustainable forms of energy. In particular, electricity generation through wind and solar systems has become increasingly important. Measures like these are undoubtedly necessary. However renewable forms of energy are coupled with an increased volatility - due to uncertain forecasts and unexpected weather events - which further increases the demand of balancing energy.

The aim of this thesis was to create a forecast of the absolute control area imbalance. To achieve that the absolute load, solar and wind forecast errors were used as explanatory variables. The challenge is, that at the time of the forecast of the absolute control area imbalance, the absolute load, solar and wind forecast errors are not known. Therefore a two-stage model was developed. In the first stage, an attempt is made to predict the absolute load, solar and wind forecast errors. Factors influencing these forecast errors are examined usinig a multiple linear regression, a tobit model (only for the solar forecast error) and a quantile regression. Then the results of the first stage (for the predicted absolute load, solar and wind forecast errors) are used as input variables for the analysis of the absolute control area imbalance in the second stage.

Unfortunately, many variables that could potentially be of interest are not publicly and freely available. These could contribute to a higher level of modelling results. In particular, there is an absence of weather- and climate-related variables. Temperature, wind speed as well as solar irradiance could provide additional explanations. As a proxy for these variables the available data from the ENTSO-E transparency platform (daily wind and solar forecasts) is used.

Those come with the advantage of (since they are aggregated values) being representative for the whole control area. Using data with a higher resolution or more specific context could also come with downsides. For example, the temperature of a rural region is not representative for the electricity consumption of a large part of the population. Furthermore, a high proportion of the electricity in Austria is generated by hydropower plants. In practice, data on storage levels and river levels will have a noticeable impact on awarded quantities of balancing energy and using these as input for the presented model could result in predictions improving accordingly. In addition, intraday prices and forecasts could also be used for short-term forecasts of the control area imbalance. Due to the fact that the forecast is made on the day before delivery, including intraday information would not only improve the forecast quality but also delay the forecast by many hours. Since this is not the focus of this thesis, the usage of intraday data is not applied.

Due to the restrictive assumptions of classical regression approaches (MLR and Tobit) an additional - optimization based - approach, namely the quantile regression (QR) was discussed. To enable a direct comparison between results of the MLR and tobit model (which look at conditional expected values) the quantile regression was limited to only use the results of considering the median (the 0.5-quantile). However, coefficients were estimated for a wide range of quantiles (in stage I). These could be incorporated into the stage II model to not only estimate the median but also predict the expected distribution of control area imbalances.

To investigate the performance of the two-stage modelling approach, the model was tested on data from 2020 while only being built on data from 2019. Not only does this ensure that the testing process is done on completely unseen and new data, but this also does not in any way unfairly benefit the developed models since 2020 was - due to COVID-19 - a year with significantly different electricity profiles (for both demand and therefore generation).

Considering the final results in table 5.11 and 5.12 the different modelling approaches can be compared regarding their performance:

Using the mentioned QR approach for stage II resulted in a reduction of the MAE (mean absolute error) of 5.5% and close to 1% increase of performance considering the RMSE (root mean square error) compared to the MLR approach. This suggests using the QR model, since it is - as mentioned before - the one that can easily be further expanded. The input values generated by stage I show no significant difference in quality - both the MLR and QR input data perform almost equally.

Three different benchmarks were defined. Comparing the stage II results of the QR against these showcases an improved performance by approximately 11% for the MAE and close to 5% for the RMSE, which shows that considering the chosen explanatory variables results in a performant model.

The topic of this thesis will become even more important in the future as the expansion of renewable energies advances and electricity consumption increases due to an increasing "electrification" of various sectors. Failures in the power grids must be avoided as far as possible. If the forecast for renewable energies (especially wind) is better, there will be fewer fluctuations in the network. Besides grid stability and security, improved forecasts and especially forecasts with lower absolute deviations from realized values will play an ever more important role, in order to also increase transparency of electricity markets and prevent potential situation of abuse (of regulatory or technical market properties) - as was outlined in the introduction.

List of Figures

List of Tables

Bibliography

[Abuella and Chowdhury, 2015] Abuella, M. and Chowdhury, B. (2015). *Solar power probabilistic forecasting by using multiple linear regression analysis.*

[Abuella and Chowdhury, 2017] Abuella, M. and Chowdhury, B. (2017). *Solar power forecasting using support vector regression.*

[Amprion, 2020] Amprion (2020). Regelreserve in Deutschland. `https://www.amprion.net/Strommarkt/Marktplattform/Regelenergie/`. [Online; accessed 06-January-2021].

[Amral et al., 2007] Amral, N., Ozveren, C., and King, D. (2007). *Short term load forecasting using multiple linear regression.*

[APG, 2020] APG (2020). Market Informations. `https://www.apg.at/markt`. [Online; accessed 05-January-2021].

[Bracale et al., 2019] Bracale, A., Caramia, P., De Falco, P., and Hong, T. (2019). *Multivariate quantile regression for short-term probabilistic load forecasting*, volume 35. IEEE.

[E-Control, 2020] E-Control (2020). Regelreserve und Ausgleichsenergie. `https://www.e-control.at/marktteilnehmer/strom/strommarkt/regelreserve-und-ausgleichsenergie`. [Online; accessed 22-February-2021].

[EconometricsAcademy, 2020] EconometricsAcademy (2020). Quantile Regression. `https://sites.google.com/site/econometricsacademy/econometrics-models/quantile-regression`. [Online; accessed 06-May-2021].

[ENTSO-E, 2020a] ENTSO-E (2020a). Installed Capacity per Production Type. `https://transparency.entsoe.eu/generation/r2/`

installedGenerationCapacityAggregation/show. [Online; accessed 11-January-2021].

[ENTSO-E, 2020b] ENTSO-E (2020b). Transparency Platform. https://transparency.entsoe.eu. [Online; accessed 05-January-2021].

[Futurezone, 2021] Futurezone (2021). Ursache für Großstörung im europäischen Stromnetz bekannt. https://futurezone.at/amp/digital-life/ursache-fuer-grossstoerung-im-europaeischen-stromnetz-bekannt/401150763. [Online; accessed 10-January-2021].

[Hurtado, 2020] Hurtado, S. I. (2020). The R BreakPoints Package. [Online; accessed 27-March-2021].

[InteressengemeinschaftWindkraft, 2020] InteressengemeinschaftWindkraft (2020). Windenergie in Österreich. https://www.igwindkraft.at/fakten. [Online; accessed 11-January-2021].

[Jansen, 2014] Jansen, M. (2014). Optimierung der Marktbedingungen für die Regelleistungserbringung durch Erneuerbare Energien. http://www.beeev.de/. [Online; accessed 07-January-2021].

[Jost et al., 2015a] Jost, D., Braun, A., Fritz, R., Drusenbaum, C., and Rohrig, K. (2015a). Dynamische Bestimmung des Regelleistungsbedarfs. *Bereich Energiewirtschaft & Netzbetrieb, Kassel*.

[Jost et al., 2015b] Jost, D., Braun, A., Fritz, R., Drusenbaum, C., and Rohrig, K. (2015b). Dynamische bestimmung des regelleistungsbedarfs. *Bereich Energiewirtschaft & Netzbetrieb, Kassel*.

[Kleiber and Zeileis, 2020] Kleiber, C. and Zeileis, A. (2020). The R AER Package. https://www.rdocumentation.org/packages/AER. [Online; accessed 28-March-2021].

[Koenker, 2021] Koenker, R. (2021). The R Quantreg Package. [Online; accessed 21-March-2021].

[Koenker and Bassett Jr, 1978] Koenker, R. and Bassett Jr, G. (1978). Regression quantiles. *Econometrica: journal of the Econometric Society*.

[Koenker and d'Orey, 1994] Koenker, R. and d'Orey, V. (1994). Remark as r92: A remark on algorithm as 229: Computing dual regression quantiles and regression rank scores. *Journal of the Royal Statistical Society. Series C (Applied Statistics)*, 43(2).

[Körbler, 2014] Körbler, J. H. (2014). Quantile Regression - Eine Anwendung auf Versicherungsleistungsdaten.

[Kraftwerke, 2020] Kraftwerke, N. (2020). Next Kraftwerke - Wissen. `https://www.next-kraftwerke.at`. [Online; accessed 05-January-2021].

[Kurscheid and Düvelmeyer, 2009] Kurscheid, E. M. and Düvelmeyer, D. (2009). *Modellierung der Inanspruchnahme positiver Minutenreserve als zusammengesetzter Poisson-Prozess mit regelzonenabhängiger Parametrierung*. Technische Universität, Fakultät für Mathematik.

[Maurer, 2010] Maurer, C. (2010). Gutachten zur dimensionierung des regelleistungsbedarfs unter dem nrv. *Consentec*.

[Möller et al., 2011] Möller, C., Rachev, S. T., Kim, Y. S., and Fabozzi, F. J. (2011). *Innovation processes in logically constrained time series*. Springer.

[R Core Team, 2013] R Core Team (2013). R: A language and environment for statistical computing.

[Röhrlich, 2019] Röhrlich, D. (2019). Unsichere Stromversorgung in Zeiten der Energiewende. `https://www.deutschlandfunk.de/ruesten-gegen-den-blackout-unsichere-stromversorgung-in.724.de.html?dram:article_id=456306`. [Online; accessed 10-January-2021].

[Sakamoto et al., 1986] Sakamoto, Y., Ishiguro, M., and Kitagawa, G. (1986). Akaike information criterion statistics. *Dordrecht, The Netherlands: D. Reidel*, 81(10.5555):26853.

[Scherrer, 2015] Scherrer, W. (2015). *Grundlagen der Ökonometrie*. Technische Universität Wien, Institut für Stochastik und Wirtschaftsmathematik.

[Schneider, 2019] Schneider, U. (2019). *Mikroökonometrie*. Technische Universität Wien, Institut für Stochastik und Wirtschaftsmathematik.

[Singhee and Wang, 2017] Singhee, A. and Wang, H. (2017). *Probabilistic forecasts of service outage counts from severe weather in a distribution grid*.

[Statista, 2020] Statista (2020). Österreich - Inlandsstromverbrauch 2019. `https://de.statista.com/`. [Online; accessed 21-February-2021].

[Team, 2012] Team, R. C. (2012). R: A language and environment for statistical computing. R Foundation for Statistical Computing. `http://www.R-project.org/`. [Online; accessed 16-March-2021].

[Tsekouras et al., 2007] Tsekouras, G., Dialynas, E., Hatziargyriou, N., and Kavatza, S. (2007). A non-linear multivariable regression model for midterm energy forecasting of power systems. *Electric Power Systems Research*, 77(12):1560–1568.

[Wan et al., 2016] Wan, C., Lin, J., Wang, J., Song, Y., and Dong, Z. Y. (2016). Direct quantile regression for nonparametric probabilistic forecasting of wind power generation. *IEEE Transactions on Power Systems*, 32(4):2767–2778.

[Wenzel, 2011] Wenzel, A. (2011). Komponentenzerlegung des regelleistungsbedarfs mit methoden der zeitreihenanalyse.

[WienEnergie, 2019] WienEnergie (2019). Entwicklung der Windkraft in Österreich. `https://positionen.wienenergie.at/beitraege/grafik-entwicklung-windkraft-oesterreich`. [Online; accessed 11-January-2021].

[Zeileis et al., 2019] Zeileis, A., Leisch, F., Hornik, K., Kleiber, C., Hansen, B., and Merkle, E. C. (2019). The R BreakPoints Package. [Online; accessed 27-March-2021].

[Österreichs E-Wirtschaft, 2018] Österreichs E-Wirtschaft (2018). Daten und Fakten zur Stromerzeugung. `https://oesterreichsenergie.at/daten-fakten-zur-stromerzeugung.html`. [Online; accessed 11-January-2021].